Duan, L., Chen, K., Tan, A. "Prestressed Concrete Bridges."
Bridge Engineering Handbook.
Ed. Wai-Fah Chen and Lian Duan
Boca Raton: CRC Press, 2000

10

Prestressed Concrete Bridges

Lian Duan
California Department of Transportation

Kang Chen
MG Engineering, Inc.

Andrew Tan
Everest International Consultants, Inc.

10.1 Introduction

Prestressed concrete structures, using high-strength materials to improve serviceability and durability, are an attractive alternative for long-span bridges, and have been used worldwide since the 1950s. This chapter focuses only on conventional prestressed concrete bridges. Segmental concrete bridges will be discussed in Chapter 11. For more detailed discussion on prestressed concrete, references are made to textbooks by Lin and Burns [1], Nawy [2], Collins and Mitchell [3].

10.1.1 Materials

10.1.1.1 Concrete

A 28-day cylinder compressive strength (f_c') of concrete 28 to 56 MPa is used most commonly in the United States. A higher early strength is often needed, however, either for the fast precast method used in the production plant or for the fast removal of formwork in the cast-in-place method. The modulus of elasticity of concrete with density between 1440 and 2500 kg/m^3 may be taken as

$$E_c = 0.043 w_c \sqrt{f_c'} \tag{10.1}$$

where w_c is the density of concrete (kg/m^3). Poisson's ratio ranges from 0.11 to 0.27, but 0.2 is often assumed.

The modulus of rupture of concrete may be taken as [4]

$$f_r = \begin{cases} 0.63\sqrt{f_c'} & \text{for normal weight concrete — flexural} \\ 0.52\sqrt{f_c'} & \text{for sand - lightweight concrete — flexural} \\ 0.44\sqrt{f_c'} & \text{for all - lightweight concrete — flexural} \\ 0.1\,f_c' & \text{for direct tension} \end{cases} \tag{10.2}$$

Concrete shrinkage is a time-dependent material behavior and mainly depends on the mixture of concrete, moisture conditions, and the curing method. Total shrinkage strains range from 0.0004 to 0.0008 over the life of concrete and about 80% of this occurs in the first year.

For moist-cured concrete devoid of shrinkage-prone aggregates, the strain due to shrinkage ε_{sh} may be estimated by [4]

$$\varepsilon_{sh} = -k_s k_h \left(\frac{t}{35+t}\right) 0.51\times 10^{-3} \tag{10.3}$$

$$K_s = \left[\frac{t}{\dfrac{26e^{0.0142(V/S)}+t}{45+t}}\right]\left[\frac{1064-3.7(V/S)}{923}\right] \tag{10.4}$$

where t is drying time (days); k_s is size factor and k_h is humidity factors may be approximated by K_n = (140-H)/70 for $H < 80\%$; K_n = 3(100-H)/70 for $H \geq 80\%$; and V/S is volume to surface area ratio. If the moist-cured concrete is exposed to drying before 5 days of curing, the shrinkage determined by Eq. (10.3) should be increased by 20%.

For stem-cured concrete devoid of shrinkage-prone aggregates:

$$\varepsilon_{sh} = -k_s k_h \left(\frac{t}{55+t}\right) 0.56\times 10^{-3} \tag{10.5}$$

Creep of concrete is a time-dependent inelastic deformation under sustained load and depends primarily on the maturity of the concrete at the time of loading. Total creep strain generally ranges from about 1.5 to 4 times that of the "instantaneous" deformation. The creep coefficient may be estimated as [4]

$$\psi(t,t_1) = 3.5K_c K_f \left(1.58 - \frac{H}{120}\right) t_i^{-0.118} \frac{(t-t_i)^{0.6}}{10+(t-t_i)^{0.6}} \tag{10.6}$$

$$K_f = \frac{62}{42+f_c'} \tag{10.7}$$

$$K_s = \left[\frac{t}{\dfrac{26e^{0.0142(V/S)}+t}{45+t}}\right]\left[\frac{1.8+1.77e^{-0.0213(V/S)}}{2.587}\right] \tag{10.8}$$

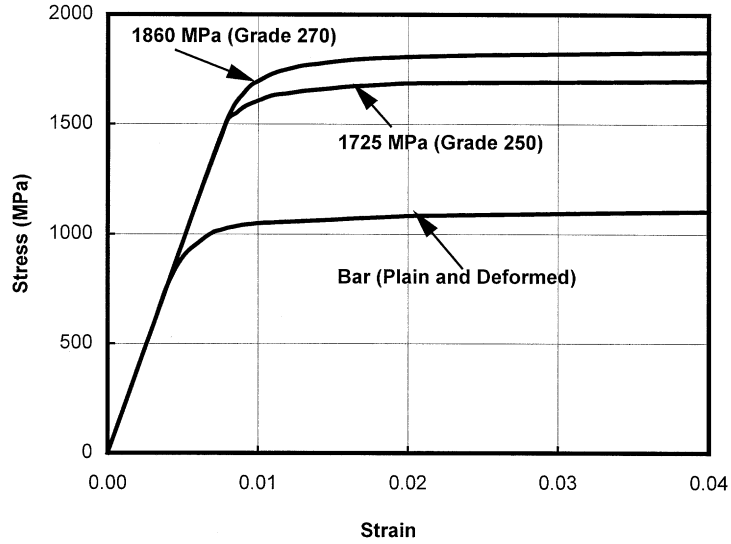

FIGURE 10.1 Typical stress–strain curves for prestressing steel.

where H is relative humidity (%); t is maturity of concrete (days); t_i is age of concrete when load is initially applied (days); K_c is the effect factor of the volume-to-surface ratio; and K_f is the effect factor of concrete strength.

Creep, shrinkage, and modulus of elasticity may also be estimated in accordance with CEB-FIP Mode Code [15].

10.1.1.2 Steel for Prestressing

Uncoated, seven-wire stress-relieved strands (AASHTO M203 or ASTM A416), or low-relaxation seven-wire strands and uncoated high-strength bars (AASHTO M275 or ASTM A722) are commonly used in prestresssed concrete bridges. Prestressing reinforcement, whether wires, strands, or bars, are also called *tendons*. The properties for prestressing steel are shown in Table 10.1.

TABLE 10.1 Properties of Prestressing Strand and Bars

Material	Grade and Type	Diameter (mm)	Tensile Strength f_{pu} (MPa)	Yield Strength f_{py} (MPa)	Modulus of Elasticity E_p (MPa)
Strand	1725 MPa (Grade 250)	6.35–15.24	1725	80% of f_{pu} except 90% of f_{pu}	197,000
	1860 MPa (Grade 270)	10.53–15.24	1860	for low relaxation strand	
Bar	Type 1, Plain	19 to 25	1035	85% of f_{pu}	
	Type 2, Deformed	15 to 36	1035	80% of f_{pu}	207,000

Typical stress–strain curves for prestressing steel are shown in Figure 10.1. These curves can be approximated by the following equations:

For Grade 250 [5]:

$$f_{ps} = \begin{cases} 197{,}000\,\varepsilon_{ps} & \text{for } \varepsilon_{ps} \le 0.008 \\ 1710 - \dfrac{0.4}{\varepsilon_{ps} - 0.006} < 0.98 f_{pu} & \text{for } \varepsilon_{ps} > 0.008 \end{cases} \tag{10.9}$$

For Grade 270 [5]:

$$f_{ps} = \begin{cases} 197{,}000\,\varepsilon_{ps} & \text{for } \varepsilon_{ps} \le 0.008 \\ 1848 - \dfrac{0.517}{\varepsilon_{ps} - 0.0065} < 0.98 f_{pu} & \text{for } \varepsilon_{ps} > 0.008 \end{cases} \tag{10.10}$$

For Bars:

$$f_{ps} = \begin{cases} 207{,}000\,\varepsilon_{ps} & \text{for } \varepsilon_{ps} \le 0.004 \\ 1020 - \dfrac{0.192}{\varepsilon_{ps} - 0.003} < 0.98 f_{pu} & \text{for } \varepsilon_{ps} > 0.004 \end{cases} \tag{10.11}$$

10.1.1.3 Advanced Composites for Prestressing

Advanced composites–fiber-reinforced plastics (FPR) with their high tensile strength and good corrosion resistance work well in prestressed concrete structures. Application of advanced composites to prestressing have been investigated since the 1950s [6–8]. Extensive research has also been conducted in Germany and Japan [9]. The Ulenbergstrasse bridge, a two-span (21.3 and 25.6 m) solid slab using 59 fiberglass tendons, was built in 1986 in Germany. It was the first prestressed concrete bridge to use advanced composite tendons in the world [10].

FPR cables and rods made of ararmid, glass, and carbon fibers embedded in a synthetic resin have an ultimate tensile strength of 1500 to 2000 MPa, with the modulus of elasticity ranging from 62,055 MPa to 165,480 MPa [9]. The main advantages of FPR are (1) a high specific strength (ratio of strength to mass density) of about 10 to 15 times greater than steel; (2) a low modulus of elasticity making the prestress loss small; (3) good performance in fatigue; tests show [11] that for CFRP, at least three times the higher stress amplitudes and higher mean stresses than steel are achieved without damage to the cable over 2 million cycles.

Although much effort has been given to exploring the use of advanced composites in civil engineering structures (see Chapter 51) and the cost of advanced composites has come down significantly, the design and construction specifications have not yet been developed. Time is still needed for engineers and bridge owners to realize the cost-effectiveness and extended life expectancy gained by using advanced composites in civil engineering structures.

10.1.1.4 Grout

For post-tensioning construction, when the tendons are to be bound, grout is needed to transfer loads and to protect the tendons from corrosion. Grout is made of water, sand, and cements or epoxy resins. AASHTO-LRFD [4] requires that details of the protection method be indicated in the contract documents. Readers are referred to the *Post-Tensioning Manual* [12].

10.1.2 Prestressing Systems

There are two types of prestressing systems: pretensioning and post-tensioning systems. Pretensioning systems are methods in which the strands are tensioned before the concrete is placed. This method is generally used for mass production of pretensioned members. Post-tensioning systems are methods in which the tendons are tensioned after concrete has reached a specified strength. This technique is often used in projects with very large elements (Figure 10.2). The main advantage of post-tensioning is its ability to post-tension both precast and cast-in-place members. Mechanical prestressing–jacking is the most common method used in bridge structures.

FIGURE 10.2 A post–tensioned box–girder bridge under construction.

10.2 Section Types

10.2.1 Void Slabs

Figure 10.3a shows FHWA [13] standard precast prestressed voided slabs. Sectional properties are listed in Table 10.2. Although the cast-in-place prestressed slab is more expensive than a reinforced concrete slab, the precast prestressed slab is economical when many spans are involved. Common spans range from 6 to 15 m. Ratios of structural depth to span are 0.03 for both simple and continuous spans.

10.2.2 I-Girders

Figures 10.3b and c show AASHTO standard I-beams [13]. The section properties are given in Table 10.3. This bridge type competes well with steel girder bridges. The formwork is complicated, particularly for skewed structures. These sections are applicable to spans 9 to 36 m. Structural depth-to-span ratios are 0.055 for simple spans and 0.05 for continuous spans.

10.2.3 Box Girders

Figure 10.3d shows FHWA [13] standard precast box sections. Section properties are given in Table 10.4. These sections are used frequently for simple spans of over 30 m and are particularly suitable for widening bridges to control deflections.

The box-girder shape shown in Figure 10.3e is often used in cast-in-place prestressed concrete bridges. The spacing of the girders can be taken as twice the depth. . This type is used mostly for spans of 30 to 180 m. Structural depth-to-span ratios are 0.045 for simple spans, and 0.04 for continuous spans. The high torsional resistance of the box girder makes it particularly suitable for curved alignment (Figure 10.4) such as those needed on freeway ramps.

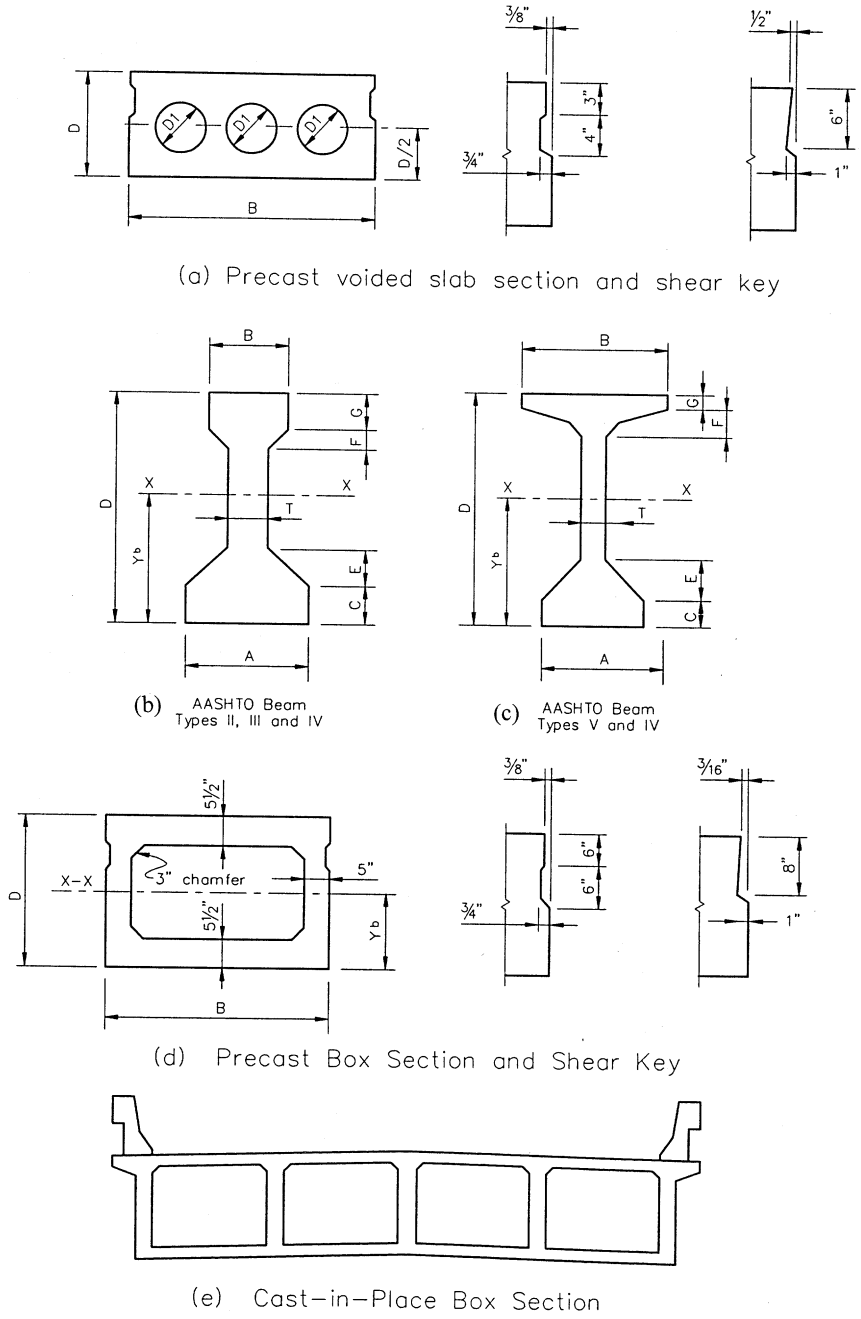

FIGURE 10.3 Typical cross sections of prestressed concrete bridge superstructures.

10.3 Losses of Prestress

Loss of prestress refers to the reduced tensile stress in the tendons. Although this loss does affect the service performance (such as camber, deflections, and cracking), it has no effect on the ultimate strength of a flexural member unless the tendons are unbounded or the final stress is less than $0.5f_{pu}$ [5]. It should be noted, however, that an accurate estimate of prestress loss is more pertinent in some prestressed concrete members than in others. Prestress losses can be divided into two categories:

TABLE 10.2 Precast Prestressed Voided Slabs Section Properties (Fig. 10.3a)

Span Range, ft (m)	Section Dimensions				Section Properties		
	Width B in. (mm)	Depth D in. (mm)	$D1$ in. (mm)	$D2$ in. (mm)	A in.^{2} (mm^2 10^6)	I_x in.^{4} (mm^4 10^9)	S_x in.^{3} (mm^3 10^6)
25	48	12	0	0	576	6,912	1,152
(7.6)	(1,219)	(305)	(0)	(0)	(0.372)	(2.877)	(18.878)
30~35	48	15	8	8	569	12,897	1,720
(10.1~10.70)	(1,219)	(381)	(203)	(203)	(0.362)	(5.368)	(28.185)
40~45	48	18	10	10	628	21,855	2,428
(12.2~13.7)	(1,219)	(457)	(254)	(254)	(0.405)	(10.097)	(310.788)
50	48	21	12	10	703	34,517	3,287
(15.2)	(1,219)	(533)	(305)	(254)	(0.454)	(1.437)	(53.864)

TABLE 10.3 Precast Prestressed I-Beam Section Properties (Figs. 10.3b and c)

AASHTO Beam Type	Section Dimensions, in. (mm)							
	Depth D	Bottom Width A	Web Width T	Top Width B	C	E	F	G
II	36 (914)	18 (457)	6 (152)	12 (305)	6 (152)	6 (152)	3 (76)	6 (152)
III	45 (1143)	22 (559)	7 (178)	16 (406)	7 (178)	7.5 (191)	4.5 (114)	7 (178)
IV	54 (1372)	26 (660)	8 (203)	20 (508)	8 (203)	9 (229)	6 (152)	8 (203)
V	65 (1651)	28 (711)	8 (203)	42 (1067)	8 (203)	10 (254)	3 (76)	5 (127)
VI	72 (1829)	28 (711)	8 (203)	42 (1067)	8 (203)	10 (254)	3 (76)	5 (127)

	Section Properties					
	A in.^{2} (mm^2 10^b)	Y_b in. (mm)	I_x in.^{4} (mm^4 10^9)	S_b in.^{3} (mm^4 10^6)	S_t in.^{3} (mm^4 10^6)	Span Ranges, ft (m)
II	369	15.83	50,980	3220	2528	40 ~ 45
	(0.2381)	(402.1)	(21.22)	(52.77)	(41.43)	(12.2 ~ 13.7)
III	560	20.27	125,390	6186	5070	50 ~ 65
	(0.3613)	(514.9)	(52.19)	(101.38)	(83.08)	(15.2 ~ 110.8)
IV	789	24.73	260,730	10543	8908	70 ~ 80
	(0.5090)	(628.1)	(108.52)	(172.77)	(145.98)	(21.4 ~ 24.4)
V	1013	31.96	521,180	16307	16791	90 ~ 100
	(0.6535)	(811.8)	(216.93)	(267.22)	(275.16)	(27.4 ~ 30.5)
VI	1085	36.38	733,340	20158	20588	110 ~ 120
	(0.7000)	(924.1)	(305.24)	(330.33)	(337.38)	(33.5 ~ 36.6)

- Instantaneous losses including losses due to anchorage set (Δf_{pA}), friction between tendons and surrounding materials (Δf_{pF}), and elastic shortening of concrete (Δf_{pES}) during the construction stage;
- Time-dependent losses including losses due to shrinkage (Δf_{pSR}), creep (Δf_{pCR}), and relaxation of the steel (Δf_{pR}) during the service life.

The total prestress loss (Δf_{pT}) is dependent on the prestressing methods.

For pretensioned members:

$$\Delta f_{pT} = \Delta f_{pES} + \Delta f_{pSR} + \Delta f_{pCR} + \Delta f_{pR} \tag{10.12}$$

For post-tensioned members:

$$\Delta f_{pT} = \Delta f_{pA} + \Delta f_{pF} + \Delta f_{pES} + \Delta f_{pSR} + \Delta f_{pCR} + \Delta f_{pR} \tag{10.13}$$

FIGURE 10.4 Prestressed box–girder bridge (I-280/110 Interchange, CA).

TABLE 10.4 Precast Prestressed Box Section Properties (Fig. 10.3d)

	Section Dimensions		Section Properties				
Span ft (m)	Width B in. (mm)	Depth D in. (mm)	A in.^{2} (mm^2 10^6)	Y_b in. (mm)	I_x in^4 (mm^4 10^9)	S_b in.^{3} (mm^3 10^6)	S_t in.^{3} (mm^3 10^6)
50	48	27	693	13.37	65,941	4,932	4,838
(15.2)	(1,219)	(686)	(0.4471)	(3310.6)	(27.447)	(80.821)	(710.281)
60	48	33	753	16.33	110,499	6,767	6,629
(18.3)	(1,219)	(838)	(0.4858)	(414.8)	(45.993)	(110.891)	(108.630)
70	48	39	813	110.29	168,367	8,728	8,524
(21.4)	(1,219)	(991)	(0.5245)	(490.0)	(70.080)	(143.026)	(1310.683)
80	48	42	843	20.78	203,088	9,773	9,571
(24.4)	(1,219)	(1,067)	(0.5439)	(527.8)	(84.532)	(160.151)	(156.841)

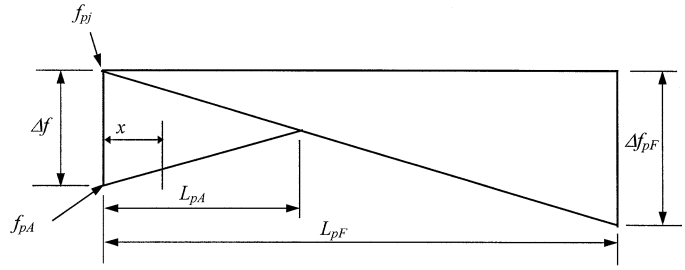

FIGURE 10.5 Anchorage set loss model.

TABLE 10.5 Friction Coefficients for Post-Tensioning Tendons

Type of Tendons and Sheathing	Wobble Coefficient K (1/mm) × (10^{-6})	Curvature Coefficient μ (1/rad)
Tendons in rigid and semirigid galvanized ducts, seven-wire strands	0.66	0.05 ~ 0.15
Pregreased tendons, wires and seven-wire strands	0.98 ~ 6.6	0.05 ~ 0.15
Mastic-coated tendons, wires and seven-wire strands	3.3 ~ 6.6	0.05 ~ 0.15
Rigid steel pipe deviations	66	0.25, lubrication required

Source: AASHTO LRFD Bridge Design Specifications, 1st Ed., American Association of State Highway and Transportation Officials. Washington, D.C. 1994. With permission.

10.3.1 Instantaneous Losses

10.3.1.1 Anchorage Set Loss

As shown in Figure 10.5, assuming that the anchorage set loss changes linearly within the length (L_{pA}), the effect of anchorage set on the cable stress can be estimated by the following formula:

$$\Delta f_{pA} = \Delta f \left(1 - \frac{x}{L_{pA}}\right) \tag{10.14}$$

$$L_{pA} = \sqrt{\frac{E\,(\Delta L)\,L_{pF}}{\Delta f_{pF}}} \tag{10.15}$$

$$\Delta f = \frac{2\,\Delta f_{pF}\,L_{pA}}{L_{pF}} \tag{10.16}$$

where ΔL is the thickness of anchorage set; E is the modulus of elasticity of anchorage set; Δf is the change in stress due to anchor set; L_{pA} is the length influenced by anchor set; L_{pF} is the length to a point where loss is known; and x is the horizontal distance from the jacking end to the point considered.

10.3.1.2 Friction Loss

For a post-tensioned member, friction losses are caused by the tendon profile *curvature effect* and the local deviation in tendon profile *wobble effects*. AASHTO-LRFD [4] specifies the following formula:

$$\Delta f_{pF} = f_{pj}\left(1 - e^{-(Kx + \mu\alpha)}\right) \tag{10.17}$$

where K is the wobble friction coefficient and μ is the curvature friction coefficient (see Table 10.5); x is the length of a prestressing tendon from the jacking end to the point considered; and α is the sum of the absolute values of angle change in the prestressing steel path from the jacking end.

10.3.1.3 Elastic Shortening Loss Δf_{pES}

The loss due to elastic shortening can be calculated using the following formula [4]:

$$\Delta f_{pES} = \begin{cases} \dfrac{E_p}{E_{ci}}\, f_{cgp} & \text{for pretensioned members} \\ \dfrac{N-1}{2N}\dfrac{E_p}{E_{ci}}\, f_{cgp} & \text{for post-tensioned members} \end{cases} \tag{10.18}$$

TABLE 10.6 Lump Sum Estimation of Time-Dependent Prestress Losses

Type of Beam Section	Level	For Wires and Strands with f_{pu} = 1620, 1725, or 1860 MPa	For Bars with f_{pu} = 1000 or 1100 MPa
Rectangular beams and solid slab	Upper bound	200 + 28 PPR	130 + 41 PPR
	Average	180 + 28 PPR	
Box girder	Upper bound	145 + 28 PPR	100
	Average	130 + 28 PPR	
I-girder	Average	$230\left[1.0-0.15\frac{f_c'-41}{41}\right]+41$ PPR	130 + 41 PPR
Single–T, double–T hollow core and voided slab	Upper bound	$230\left[1.0-0.15\frac{f_c'-41}{41}\right]+41$ PPR	$230\left[1.0-0.15\frac{f_c'-41}{41}\right]+41$ PPR
	Average	$230\left[1.0-0.15\frac{f_c'-41}{41}\right]+41$ PPR	

Note:
1. PPR is partial prestress ratio = $(A_{ps}f_{py})/(A_{ps}f_{py} + A_sf_y)$.
2. For low-relaxation strands, the above values may be reduced by
   - 28 MPa for box girders
   - 41 MPa for rectangular beams, solid slab and I-girders, and
   - 55 MPa for single–T, double–T, hollow–core and voided slabs.

Source: AASHTO LRFD Bridge Design Specifications, 1st Ed., American Association of State Highway and Transportation Officials. Washington, D.C. 1994. With permission.

where E_{ci} is modulus of elasticity of concrete at transfer (for pretensioned members) or after jacking (for post-tensioned members); N is the number of identical prestressing tendons; and f_{cgp} is sum of the concrete stress at the center of gravity of the prestressing tendons due to the prestressing force at transfer (for pretensioned members) or after jacking (for post-tensioned members) and the self-weight of members at the section with the maximum moment. For post-tensioned structures with bonded tendons, f_{cgp} may be calculated at the center section of the span for simply supported structures, at the section with the maximum moment for continuous structures.

10.3.2 Time-Dependent Losses

10.3.2.1 Lump Sum Estimation

AASHTO-LRFD [4] provides the approximate lump sum estimation (Table 10.6) of time-dependent loses Δf_{pTM} resulting from shrinkage and creep of concrete, and relaxation of the prestressing steel. While the use of lump sum losses is acceptable for "average exposure conditions," for unusual conditions, more-refined estimates are required.

10.3.2.2 Refined Estimation

a. *Shrinkage Loss*: Shrinkage loss can be determined by formulas [4]:

$$\Delta f_{pSR} = \begin{cases} 93 - 0.85H & \text{for pretensioned members} \\ 11 - 1.03H & \text{for post-tensioned members} \end{cases} \tag{10.19}$$

where H is average annual ambient relative humidity (%).

b. *Creep Loss*: Creep loss can be predicted by [4]:

$$\Delta f_{pCR} = 12 f_{cgp} - 7\Delta f_{cdp} \geq 0 \tag{10.20}$$

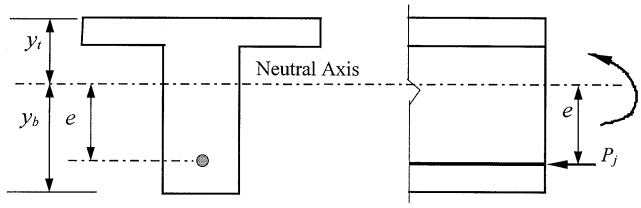

FIGURE 10.6 Prestressed concrete member section at Service Limit State.

where f_{cgp} is concrete stress at center of gravity of prestressing steel at transfer, and Δf_{cdp} is concrete stress change at center of gravity of prestressing steel due to permanent loads, except the load acting at the time the prestressing force is applied.

c. *Relaxation Loss*: The total relaxation loss (Δf_{pR}) includes two parts: relaxation at time of transfer Δf_{pR1} and after transfer Δf_{pR2}. For a pretensioned member initially stressed beyond 0.5 f_{pu}, AASHTO-LRFD [4] specifies

$$\Delta f_{pR1} = \begin{cases} \dfrac{\log 24t}{10}\left[\dfrac{f_{pi}}{f_{py}} - 0.55\right] f_{pi} & \text{for stress-relieved strand} \\ \dfrac{\log 24t}{40}\left[\dfrac{f_{pi}}{f_{py}} - 0.55\right] f_{pi} & \text{for low-relaxation strand} \end{cases} \tag{10.21}$$

For stress-relieved strands

$$\Delta f_{pR2} = \begin{cases} 138 - 0.4\Delta f_{pES} - 0.2(\Delta f_{pSR} + \Delta f_{pCR}) & \text{for pretensioning} \\ 138 - 0.3\Delta f_{pF} - 0.4\Delta f_{pES} - 0.2(\Delta f_{pSR} + \Delta f_{pCR}) & \text{for post-tensioning} \end{cases} \tag{10.22}$$

where t is time estimated in days from testing to transfer. For low-relaxation strands, Δf_{pR2} is 30% of those values obtained from Eq. (10.22).

10.4 Design Considerations

10.4.1 Basic Theory

Compared with reinforced concrete, the main distinguishing characteristics of prestressed concrete are that

- The stresses for concrete and prestressing steel and deformation of structures at each stage, i.e., during prestressing, handling, transportation, erection, and the service life, as well as stress concentrations, need to be investigated on the basis of elastic theory.
- The prestressing force is determined by concrete stress limits under service load.
- Flexure and shear capacities are determined based on the ultimate strength theory.

For the prestressed concrete member section shown in Figure 10.6, the stress at various load stages can be expressed by the following formula:

$$f = \frac{P_j}{A} \pm \frac{P_j e y}{I} \pm \frac{My}{I} \tag{10.23}$$

TABLE 10.7 Stress Limits for Prestressing Tendons

Stress Type	Prestressing Method	Prestressing Tendon Type: Stress Relieved Strand and Plain High-Strength Bars	Prestressing Tendon Type: Low Relaxation Strand	Prestressing Tendon Type: Deformed High-Strength Bars
At jacking, f_{pj}	Pretensioning	$0.72f_{pu}$	$0.78f_{pu}$	—
	Post-tensioning	$0.76f_{pu}$	$0.80f_{pu}$	$0.75f_{pu}$
After transfer, f_{pt}	Pretensioning	$0.70f_{pu}$	$0.74f_{pu}$	—
	Post-tensioning — at anchorages and couplers immediately after anchor set	$0.70f_{pu}$	$0.70f_{pu}$	$0.66f_{pu}$
	Post-tensioning — general	$0.70f_{pu}$	$0.74f_{pu}$	$0.66f_{pu}$
At Service Limit State, f_{pc}	After all losses	$0.80f_{py}$	$0.80f_{py}$	$0.80f_{py}$

Source: AASHTO LRFD Bridge Design Specifications, 1st Ed., American Association of State Highway and Transportation Officials. Washington, D.C. 1994. With permission.

TABLE 10.8 Temporary Concrete Stress Limits at Jacking State before Losses due to Creep and Shrinkage — Fully Prestressed Components

Stress Type	Area and Condition	Stress (MPa)
Compressive	Pretensioned	$0.60\ f'_{ci}$
	Post-tensioned	$0.55\ f'_{ci}$
Tensile	Precompressed tensile zone without bonded reinforcement	N/A
	Area other than the precompressed tensile zones and without bonded auxiliary reinforcement	$0.25\sqrt{f'_{ci}} \le 1.38$
	Area with bonded reinforcement which is sufficient to resist 120% of the tension force in the cracked concrete computed on the basis of uncracked section	$0.58\sqrt{f'_{ci}}$
	Handling stresses in prestressed piles	$0.415\sqrt{f'_{ci}}$

Note: Tensile stress limits are for nonsegmental bridges only.
Source: AASHTO LRFD Bridge Design Specifications, 1st Ed., American Association of State Highway and Transportation Officials. Washington, D.C. 1994. With permission.

where P_j is the prestress force; A is the cross-sectional area; I is the moment of inertia; e is the distance from the center of gravity to the centroid of the prestressing cable; y is the distance from the centroidal axis; and M is the externally applied moment.

Section properties are dependent on the prestressing method and the load stage. In the analysis, the following guidelines may be useful:

- Before bounding of the tendons, for a post-tensioned member, the net section should be used theoretically, but the gross section properties can be used with a negligible tolerance.
- After bounding of tendons, the transformed section should be used, but gross section properties may be used approximately.
- At the service load stage, transformed section properties should be used.

10.4.2 Stress Limits

The stress limits are the basic requirements for designing a prestressed concrete member. The purpose for stress limits on the prestressing tendons is to mitigate tendon fracture, to avoid inelastic tendon deformation, and to allow for prestress losses. Tables 10.7 lists the AASHTO-LRFD [4] stress limits for prestressing tendons.

TABLE 10.9 Concrete Stress Limits at Service Limit State after All Losses — Fully Prestressed Components

Stress Type	Area and Condition		Stress (MPa)
Compressive	Nonsegmental bridge at service stage		$0.45\,f_c'$
	Nonsegmental bridge during shipping and handling		$0.60\,f_c'$
	Segmental bridge during shipping and handling		$0.45\,f_c'$
Tensile	Precompressed tensile zone assuming uncracked section	With bonded prestressing tendons other than piles	$0.50\sqrt{f_c'}$
		Subjected to severe corrosive conditions	$0.25\sqrt{f_c'}$
		With unbonded prestressing tendon	No tension

Note: Tensile stress limits are for nonsegmental bridges only.
Source: AASHTO LRFD Bridge Design Specifications, 1st Ed., American Association of State Highway and Transportation Officials. Washington, D.C. 1994. With permission.

The purpose for stress limits on the concrete is to ensure no overstressing at jacking and after transfer stages and to avoid cracking (fully prestressed) or to control cracking (partially prestressed) at the service load stage. Tables 10.8 and 10.9 list the AASHTO-LRFD [4] stress limits for concrete.

A prestressed member that does not allow cracking at service loads is called a fully prestressed member, whereas one that does is called a partially prestressed member. Compared with full prestress, partial prestress can minimize camber, especially when the dead load is relatively small, as well as provide savings in prestressing steel, in the work required to tension, and in the size of end anchorages and utilizing cheaper mild steel. On the other hand, engineers must be aware that partial prestress may cause earlier cracks and greater deflection under overloads and higher principal tensile stresses under service loads. Nonprestressed reinforcement is often needed to provide higher flexural strength and to control cracking in a partially prestressed member.

10.4.3 Cable Layout

A cable is a group of prestressing tendons and the center of gravity of all prestressing reinforcement. It is a general design principle that the maximum eccentricity of prestressing tendons should occur at locations of maximum moments. Although straight tendons (Figure 10.7a) and harped multi-straight tendons (Figure 10.7b and c) are common in the precast members, curved tendons are more popular for cast-in-place post-tensioned members. Typical cable layouts for bridge superstructures are shown in Figure 10.7.

To ensure that the tensile stress in extreme concrete fibers under service does not exceed code stress limits [4, 14], cable layout envelopes are delimited. Figure 10.8 shows limiting envelopes for simply supported members. From Eq. (10.23), the stress at extreme fiber can be obtained

$$f = \frac{P_j}{A} \pm \frac{P_j eC}{I} \pm \frac{MC}{I} \tag{10.24}$$

where C is the distance of the top or bottom extreme fibers from the center gravity of the section (y_b or y_t as shown in Figure 10.6).

When no tensile stress is allowed, the limiting eccentricity envelope can be solved from Eq. (10.24) with

$$e_{limit} = \frac{I}{AC} \pm \frac{M}{IP_j} \tag{10.25}$$

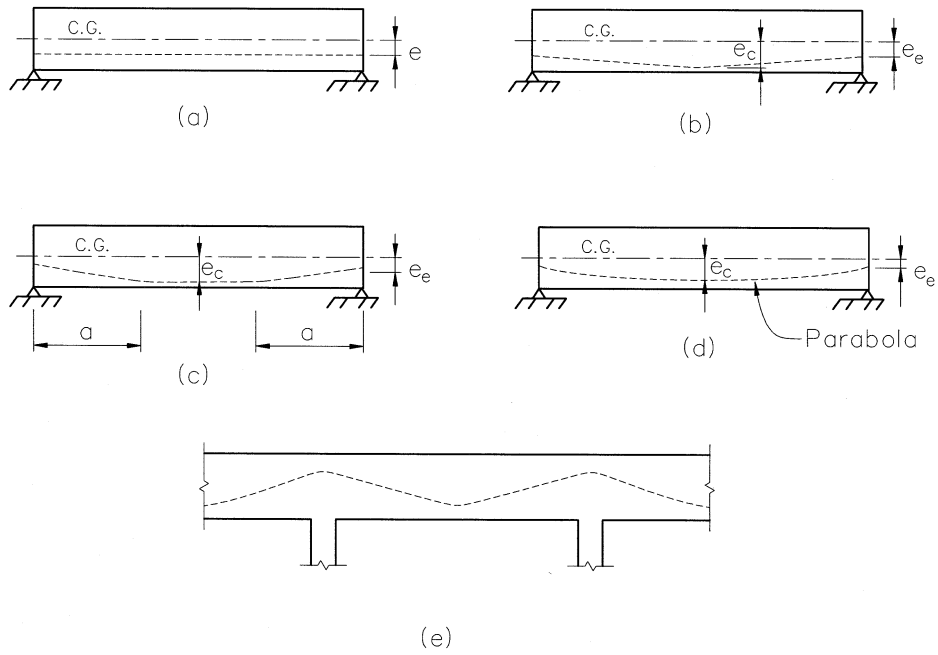

FIGURE 10.7 Cable layout for bridge superstructures.

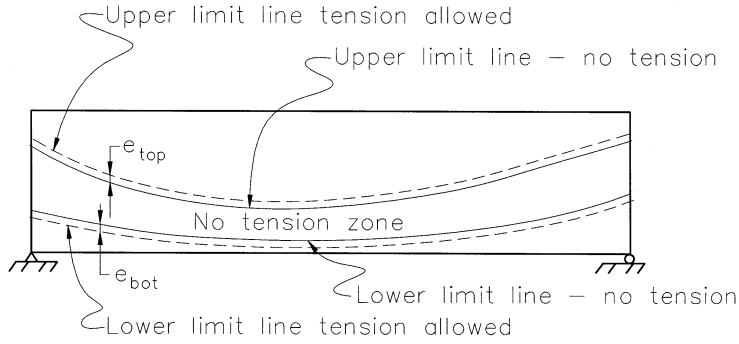

FIGURE 10.8 Cable layout envelopes.

For limited tension stress f_t, additional eccentricities can be obtained:

$$e' = \frac{f_t I}{P_j C} \tag{10.26}$$

10.4.4 Secondary Moments

The primary moment ($M_1 = P_j e$) is defined as the moment in the concrete section caused by the eccentricity of the prestress for a statically determinate member. The secondary moment M_s (Figure 10.9d) is defined as moment induced by prestress and structural continuity in an indeterminate member. Secondary moments can be obtained by various methods. The resulting moment is simply the sum of the primary and secondary moments.

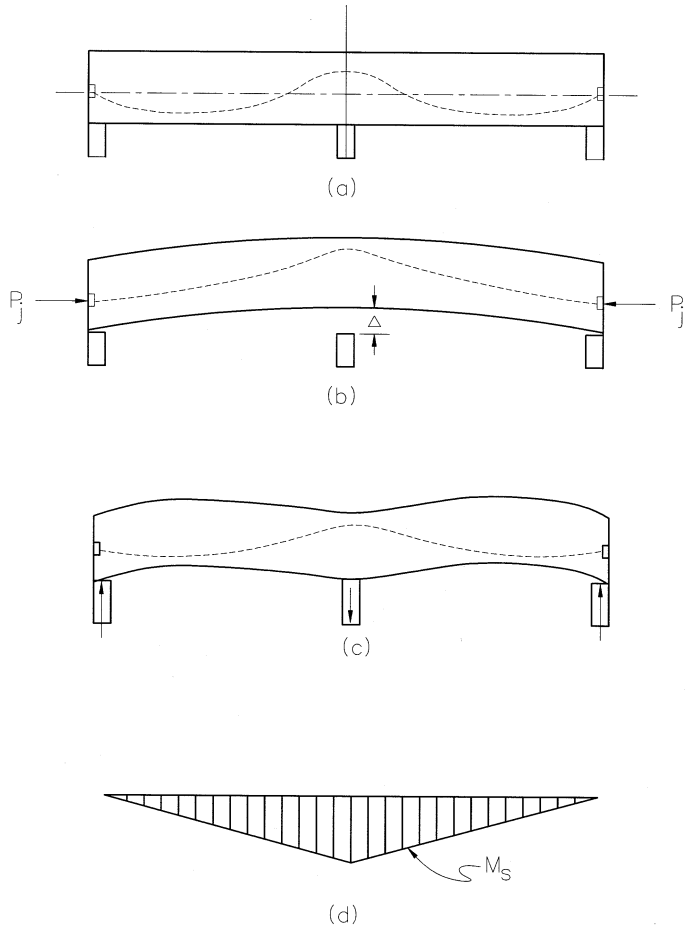

FIGURE 10.9 Secondary moments.

10.4.5 Flexural Strength

Flexural strength is based on the following assumptions [4]:

- For members with bonded tendons, strain is linearly distributed across a section; for members with unbonded tendons, the total change in tendon length is equal to the total change in member length over the distance between two anchorage points.
- The maximum usable strain at extreme compressive fiber is 0.003.
- The tensile strength of concrete is neglected.
- A concrete stress of 0.85 f_c' is uniformly distributed over an equivalent compression zone.
- Nonprestressed reinforcement reaches the yield strength, and the corresponding stresses in the prestressing tendons are compatible based on plane section assumptions.

For a member with a flanged section (Figure 10.10) subjected to uniaxial bending, the equations of equilibrium are used to give a nominal moment resistance of

$$M_n = A_{ps} f_{ps}\left(d_p - \frac{a}{2}\right) + A_s f_y\left(d_s - \frac{a}{2}\right) - A_s' f_y'\left(d_s' - \frac{a}{2}\right) + 0.85 f_c'(b - b_w)\beta_1 h_f\left(\frac{a}{2} - \frac{h_f}{2}\right) \quad (10.27)$$

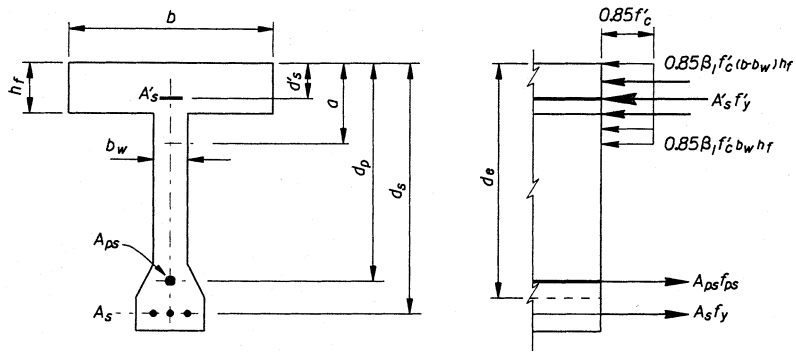

FIGURE 10.10 A flanged section at nominal moment capacity state.

$$a = \beta_1 c \tag{10.28}$$

For bonded tendons:

$$c = \frac{A_{ps} f_{pu} + A_s f_y - A'_s f'_y - 0.85\beta_1 f'_c (b - b_w)h_f}{0.85\beta_1 f'_c b_w + kA_{ps}\dfrac{f_{pu}}{d_p}} \geq h_f \tag{10.29}$$

$$f_{ps} = f_{pu}\left(1 - k\frac{c}{d_p}\right) \tag{10.30}$$

$$k = 2\left(1.04 - \frac{f_{py}}{f_{pu}}\right) \tag{10.31}$$

$$0.85 \geq \beta_1 = 0.85 - \frac{(f'_c - 28)(0.05)}{7} \geq 0.65 \tag{10.32}$$

where A represents area; f is stress; b is the width of the compression face of member; b_w is the web width of a section; h_f is the compression flange depth of the cross section; d_p and d_s are distances from extreme compression fiber to the centroid of prestressing tendons and to centroid of tension reinforcement, respectively; subscripts c and y indicate specified strength for concrete and steel, respectively; subscripts p and s mean prestressing steel and reinforcement steel, respectively; subscripts ps, py, and pu correspond to states of nominal moment capacity, yield, and specified tensile strength of prestressing steel, respectively; superscript $'$ represents compression. The above equations also can be used for rectangular section in which $b_w = b$ is taken.

For unbound tendons:

$$c = \frac{A_{ps} f_{pu} + A_s f_y - A'_s f'_y - 0.85\beta_1 f'_c (b - b_w)h_f}{0.85\beta_1 f'_c b_w} \geq h_f \tag{10.33}$$

$$f_{ps} = f_{pe} + \Omega_u E_p \varepsilon_{cu}\left(\frac{d_p}{c} - 1.0\right)\frac{L_1}{L_2} \leq 0.94 f_{py} \tag{10.34}$$

where L_1 is length of loaded span or spans affected by the same tendons; L_2 is total length of tendon between anchorage; Ω_u is the bond reduction coefficient given by

$$\Omega_u = \begin{cases} \dfrac{3}{L/d_p} & \text{for uniform and near third point loading} \\ \dfrac{1.5}{L/d_p} & \text{for near midspan loading} \end{cases} \tag{10.35}$$

in which L is span length.

Maximum reinforcement limit:

$$\frac{c}{d_e} \le 0.42 \tag{10.36}$$

$$d_e = \frac{A_{ps} f_{ps} d_p + A_s f_y d_s}{A_{ps} f_{ps} + A_s f_y} \tag{10.37}$$

Minimum reinforcement limit:

$$\phi M_n \ge 1.2\ M_{cr} \tag{10.38}$$

in which ϕ is flexural resistance factor 1.0 for prestressed concrete and 0.9 for reinforced concrete; M_{cr} is the cracking moment strength given by the elastic stress distribution and the modulus of rupture of concrete.

$$M_{cr} = \frac{I}{y_t}\left(f_r + f_{pe} - f_d\right) \tag{10.39}$$

where f_{pe} is compressive stress in concrete due to effective prestresses; and f_d is stress due to unfactored self-weight; both f_{pe} and f_d are stresses at extreme fiber where tensile stresses are produced by externally applied loads.

10.4.6 Shear Strength

The shear resistance is contributed by the concrete, the transverse reinforcement and vertical component of prestressing force. The modified compression field theory-based shear design strength [3] was adopted by the AASHTO-LRFD [4] and has the formula:

$$V_n = \text{the lesser of} \begin{cases} V_c + V_s + V_p \\ 0.25 f_c' b_v d_v + V_p \end{cases} \tag{10.40}$$

where

$$V_c = 0.083 \beta \sqrt{f_c'}\, b_v\, d_v \tag{10.41}$$

$$V_s = \frac{A_v f_y d_v (\cos\theta + \cot\alpha)\sin\alpha}{s} \tag{10.42}$$

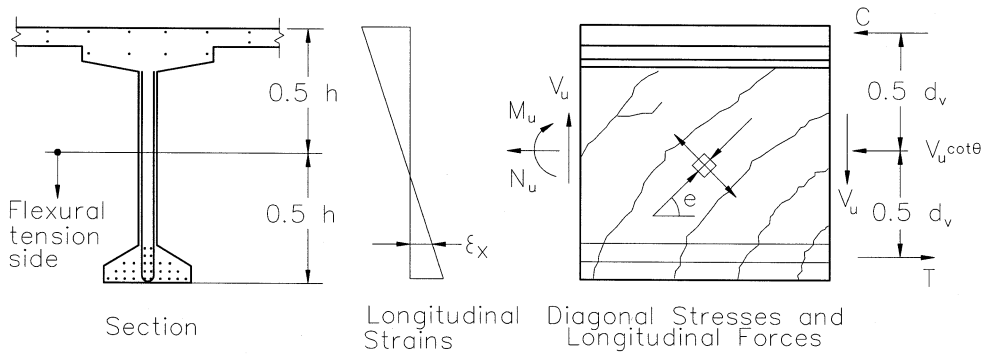

FIGURE 10.11 Illustration of A_c for shear strength calculation. (*Source*: AASHTO LRFD Bridge Design Specifications, 1st Ed., American Association of State Highway and Transportation Officials. Washington, D.C. 1994. With permission.)

TABLE 10.10 Values of θ and β for Sections with Transverse Reinforcement

$\frac{v}{f'_c}$	Angle (degree)	$\varepsilon_x \times 1000$										
		–.02	–0.15	–0.1	0	0.125	0.25	0.50	0.75	1.00	1.50	2.00
≤ 0.05	θ	27.0	27.0	27.0	27.0	27.0	28.5	29.0	33.0	36.0	41.0	43.0
	β	6.78	6.17	5.63	4.88	3.99	3.49	2.51	2.37	2.23	1.95	1.72
0.075	θ	27.0	27.0	27.0	27.0	27.0	27.5	30.0	33.5	36.0	40.0	42.0
	β	6.78	6.17	5.63	4.88	3.65	3.01	2.47	2.33	2.16	1.90	1.65
0.100	θ	23.5	23.5	23.5	23.5	24.0	26.5	30.5	34.0	36.0	38.0	39.0
	β	6.50	5.87	5.31	3.26	2.61	2.54	2.41	2.28	2.09	1.72	1.45
0.127	θ	20.0	21.0	22.0	23.5	26.0	28.0	31.5	34.0	36.0	37.0	38.0
	β	2.71	2.71	2.71	2.60	2.57	2.50	2.37	2.18	2.01	1.60	1.35
0.150	θ	22.0	22.5	23.5	25.0	27.0	29.0	32.0	34.0	36.0	36.5	37.0
	β	2.66	2.61	2.61	2.55	2.50	2.45	2.28	2.06	1.93	1.50	1.24
0.175	θ	23.5	24.0	25.0	26.5	28.0	30.0	32.5	34.0	35.0	35.5	36.0
	β	2.59	2.58	2.54	2.50	2.41	2.39	2.20	1.95	1.74	1.35	1.11
0.200	θ	25.0	25.5	26.5	27.5	29.0	31.0	33.0	34.0	34.5	35.0	36.0
	β	2.55	2.49	2.48	2.45	2.37	2.33	2.10	1.82	1.58	1.21	1.00
0.225	θ	26.5	27.0	27.5	29.0	30.5	32.0	33.0	34.0	34.5	36.5	39.0
	β	2.45	2.38	2.43	2.37	2.33	2.27	1.92	1.67	1.43	1.18	1.14
0.250	θ	28.0	28.5	29.0	30.0	31.0	32.0	33.0	34.0	35.5	38.5	41.5
	β	2.36	2.32	2.36	2.30	2.28	2.01	1.64	1.52	1.40	1.30	1.25

(*Source*: AASHTO LRFD Bridge Design Specifications, 1st Ed., American Association of State Highway and Transportation Officials. Washington, D.C. 1994. With permission.)

where b_v is the effective web width determined by subtracting the diameters of ungrouted ducts or one half the diameters of grouted ducts; d_v is the effective depth between the resultants of the tensile and compressive forces due to flexure, but not to be taken less than the greater of $0.9d_e$ or $0.72h$; A_v is the area of transverse reinforcement within distance s; s is the spacing of stirrups; α is the angle of inclination of transverse reinforcement to longitudinal axis; β is a factor indicating ability of diagonally cracked concrete to transmit tension; θ is the angle of inclination of diagonal compressive stresses (Figure 10.11). The values of β and θ for sections with transverse reinforcement are given in Table 10.10. In using this table, the shear stress v and strain ε_x in the reinforcement on the flexural tension side of the member are determined by

$$v = \frac{V_u - \phi V_p}{\phi b_v d_v} \tag{10.43}$$

$$\varepsilon_x = \frac{\frac{M_u}{d_v} + 0.5N_u + 0.5V_u \cot\theta - A_{ps} f_{po}}{E_s A_s + E_p A_{ps}} \leq 0.002 \tag{10.44}$$

where M_u and N_u are factored moment and axial force (taken as positive if compressive) associated with V_u and f_{po} is stress in prestressing steel when the stress in the surrounding concrete is zero and can be conservatively taken as the effective stress after losses f_{pe}. When the value of ε_x calculated from the above equation is negative, its absolute value shall be reduced by multiplying by the factor F_ε, taken as

$$F_\varepsilon = \frac{E_s A_s + E_p A_{ps}}{E_c A_c + E_s A_s + E_p A_{ps}} \tag{10.45}$$

where E_s, E_p, and E_c are modulus of elasticity for reinforcement, prestressing steel, and concrete, respectively; A_c is area of concrete on the flexural tension side of the member as shown in Figure 10.11.

Minimum transverse reinforcement:

$$A_{v\min} = 0.083\sqrt{f_c'}\,\frac{b_v s}{f_y} \tag{10.46}$$

Maximum spacing of transverse reinforcement:

$$\text{For } V_u < 0.1 f_c' b_v d_v \qquad s_{\max} = \text{the smaller of} \begin{cases} 0.8 d_v \\ 600 \text{ mm} \end{cases} \tag{10.47}$$

$$\text{For } V_u \geq 0.1 f_c' b_v d_v \qquad s_{\max} = \text{the smaller of} \begin{cases} 0.4 d_v \\ 300 \text{ mm} \end{cases} \tag{10.48}$$

10.4.7 Camber and Deflections

As opposed to load deflection, camber is usually referred to as reversed deflection and is caused by prestressing. A careful evaluation of camber and deflection for a prestressed concrete member is necessary to meet serviceability requirements. The following formulas developed by the moment–area method can be used to estimate midspan immediate camber for simply supported members as shown in Figure 10.7.

For straight tendon (Figure 10.7a):

$$\Delta = \frac{L^2}{8E_c I} M_e \tag{10.49}$$

For one-point harping tendon (Figure 10.7b):

$$\Delta = \frac{L^2}{8E_c I}\left(M_c + \frac{2}{3} M_e\right) \tag{10.50}$$

For two-point harping tendon (*Figure 10.7c*):

$$\Delta = \frac{L^2}{8E_cI}\left(M_c + M_e - \frac{M_e}{3}\left(\frac{2a}{L}\right)^2\right) \tag{10.51}$$

For parabola tendon (*Figure 10.7d*):

$$\Delta = \frac{L^2}{8E_cI}\left(M_e + \frac{5}{6}M_c\right) \tag{10.52}$$

where M_e is the primary moment at end, $P_j e_{\text{end}}$, and M_c is the primary moment at midspan $P_j e_c$. Uncracked gross section properties are often used in calculating camber. For deflection at service loads, cracked section properties, i.e., moment of inertia I_{cr}, should be used at the post-cracking service load stage. It should be noted that long term effect of creep and shrinkage shall be considered in the final camber calculations. In general, final camber may be assumed 3 times as great as immediate camber.

10.4.8 Anchorage Zones

In a pretensioned member, prestressing tendons transfer the compression load to the surrounding concrete over a length L_t gradually. In a post-tensioned member, prestressing tendons transfer the compression directly to the end of the member through bearing plates and anchors. The anchorage zone, based on the principle of St. Venant, is geometrically defined as the volume of concrete through which the prestressing force at the anchorage device spreads transversely to a more linear stress distribution across the entire cross section at some distance from the anchorage device [4].

For design purposes, the anchorage zone can be divided into general and local zones [4]. The region of tensile stresses is the general zone. The region of high compressive stresses (immediately ahead of the anchorage device) is the local zone. For the design of the general zone, a "strut-and-tie model," a refined elastic stress analysis or approximate methods may be used to determine the stresses, while the resistance to bursting forces is provided by reinforcing spirals, closed hoops, or anchoraged transverse ties. For the design of the local zone, bearing pressure is a major concern. For detailed requirements, see AASHTO-LRFD [4].

10.5 Design Example

Two-Span Continuous Cast-in-Place Box-Girder Bridge

Given

A two-span continuous cast-in-place prestressed concrete box-girder bridge has two equal spans of length 48 m with a single-column bent. The superstructure is 10.4 m wide. The elevation view of the bridge is shown in Figure 10.12a.

Material:

Initial concrete: $f'_{ci} = 24$ MPa , $E_{ci} = 24{,}768$ MPa
Final concrete: $f'_c = 28$ MPa , $E_c = 26{,}752$ MPa
Prestressing steel: $f_{pu} = 1860$ MPa low relaxation strand, $E_p = 197{,}000$ MPa
Mild steel: $f_y = 400$ MPa, $E_s = 200{,}000$ MPa

Prestressing:

Anchorage set thickness = 10 mm
Prestressing stress at jacking $f_{pj} = 0.8\, f_{pu} = 1488$ MPa
The secondary moments due to prestressing at the bent are $M_{DA} = 1.118\, P_j$, $M_{DG} = 1.107\, P_j$

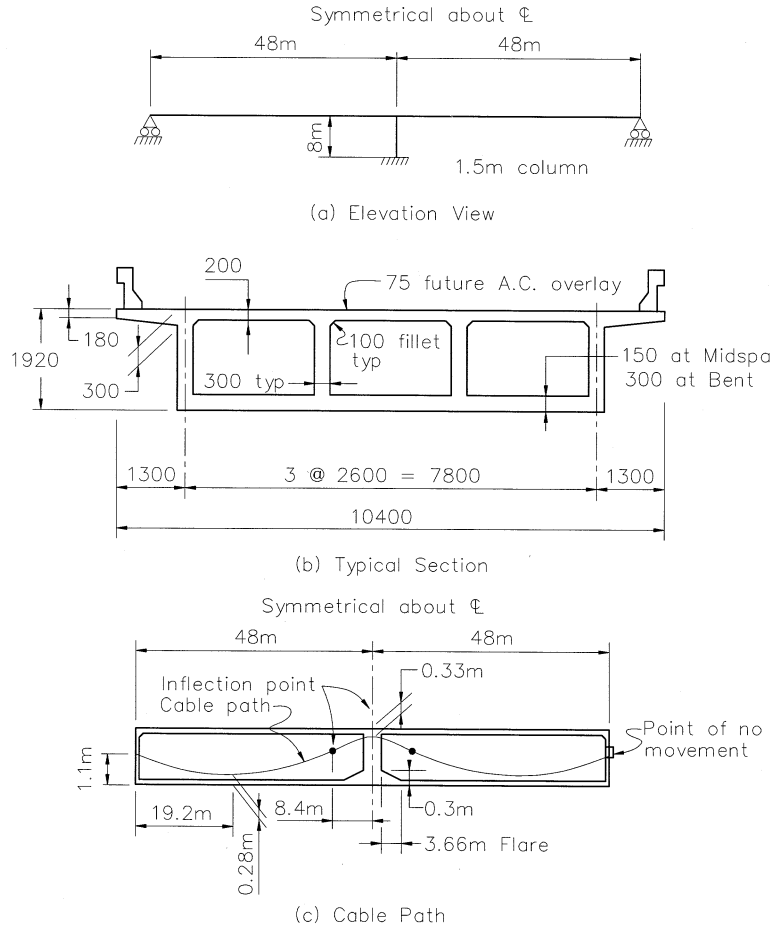

FIGURE 10.12 A two–span continuous prestressed concrete box–girder bridge.

Loads:

Dead Load = self-weight + barrier rail + future wearing 75 mm AC overlay
Live Load = AASHTO HL-93 Live Load + dynamic load allowance

Specification:

AASHTO-LRFD [4] (referred as AASHTO in this example)

Requirements

1. Determine cross section geometry
2. Determine longitudinal section and cable path
3. Calculate loads
4. Calculate live load distribution factors for interior girder
5. Calculate unfactored moment and shear demands for interior girder
6. Determine load factors for Strength Limit State I and Service Limit State I
7. Calculate section properties for interior girder
8. Calculate prestress losses
9. Determine prestressing force P_j for interior girder

10. Check concrete strength for interior girder — Service Limit State I
11. Flexural strength design for interior girder — Strength Limit State I
12. Shear strength design for interior girder — Strength Limit State I

Solution

1. Determine Cross Section Geometry

a. *Structural depth — d*:
For prestressed continuous spans, the structural depth d can be determined using a depth-to-span ratio (d/L) of 0.04 (AASHTO LRFD Table 2.5.2.6.3-1).

$$d = 0.04L = 0.04(48) = 1.92 \text{ m}$$

b. *Girder spacing — S*:
The spacing of girders is generally taken no more than twice their depth.

$$S_{max} < 2\ d = 2\ (1.92) = 3.84 \text{ m}$$

By using an overhang of 1.2 m, the center-to-center distance between two exterior girders is 10.4 m – (2)(1.2 m) = 8 m.

Try three girders and two bays, $S = 8 \text{ m}/2 = 4 \text{ m} > 3.84 \text{ m}$ NG
Try four girders and three bays, $S = 8 \text{ m}/3 = 2.67 \text{ m} < 3.84 \text{ m}$ OK
Use a girder spacing $S = 2.6$ m

c. *Typical section*:
From past experience and design practice, we select that a thickness of 180 mm at the edge and 300 mm at the face of exterior girder for the overhang. The web thickness is chosen to be 300 mm at normal section and 450 mm at the anchorage end. The length of the flare is usually taken as 1/10 of the span length, say 4.8 m. The deck and soffit thickness depends on the clear distance between adjacent girders; 200 and 150 mm are chosen for the deck and soffit thickness, respectively. The selected box-girder section configurations for this example are shown in Figure 10.12b. The section properties of the box girder are as follows:

Properties	Midspan	Bent (face of support)
A (m^2)	5.301	6.336
I (m^4)	2.844	3.513
y_b (m)	1.102	0.959

2. Determine Longitudinal Section and Cable Path

To lower the center of gravity of the superstructure at the face of the bent cap in the CIP post-tensioned box girder, the thickness of soffit is flared to 300 mm as shown in Figure 10.12c. A cable path is generally controlled by the maximum dead-load moment and the position of the jack at the end section. Maximum eccentricities should occur at points of maximum dead load moments and almost no eccentricity should be present at the jacked end section. For this example, the maximum dead-load moments occur at three locations: at the bent cap, at the locations close to $0.4L$ for Span 1 and $0.6L$ for Span 2. A parabolic cable path is chosen as shown in Figure 10.12c.

3. Calculate Loads

a. *Component dead load — DC*:
The component dead load *DC* includes all structural dead loads with the exception of the future wearing surface and specified utility loads. For design purposes, two parts of the *DC* are defined as:

*DC*1 — girder self-weight (density 2400 kg/m^3) acting at the prestressing stage
*DC*2 — barrier rail weight (11.5 kN/m) acting at service stage after all losses.

b. *Wearing surface load — DW*:
The future wearing surface of 75 mm with a density 2250 kg/m^3

DW = (deck width – barrier width) (thickness of wearing surface) (density)
= [10.4 m – 2(0.54 m)](0.075 m)(2250 kg/m^3)(9.8066 m/s^2) = 15,423 N/m
= 15.423 kN/m

c. *Live-Load LL and Dynamic Load Allowance — IM*:
The design live load *LL* is the AASHTO HL-93 vehicular live loading. To consider the wheel-load impact from moving vehicles, the dynamic load allowance IM = 33% [AASHTO LRFD Table 3.6.2.1-1] is applied to the design truck.

4. Calculate Live Load Distribution Factors
AASHTO [1994] recommends that approximate methods be used to distribute live load to individual girders (AASHTO-LRFD 4.6.2.2.2). The dimensions relevant to this prestressed box girder are: depth d = 1920 mm, number of cells N_c = 3, spacing of girders S = 2600 mm, span length L = 48,000 mm, half of the girder spacing plus the total overhang W_e = 2600 mm, and the distance between the center of an exterior girder and the interior edge of a barrier d_e = 1300 – 535 = 765 m. This box girder is within the range of applicability of the AASHTO approximate formulas. The live-load distribution factors are calculated as follows:

a. *Live-load distribution factor for bending moments*:
i. Interior girder (AASHTO Table 4.6.2.2.2b-1):
• One design lane loaded:

$$g_M = \left(1.75+\frac{S}{1100}\right)\left(\frac{300}{L}\right)^{0.35}\left(\frac{1}{N_c}\right)^{0.45}$$

$$= \left(1.75+\frac{2600}{1100}\right)\left(\frac{300}{48,000}\right)^{0.35}\left(\frac{1}{3}\right)^{0.45} = 0.425 \text{ lanes}$$

• Two or more design lanes loaded:

$$g_M = \left(\frac{13}{N_c}\right)^{0.3}\left(\frac{S}{430}\right)\left(\frac{1}{L}\right)^{0.25}$$

$$= \left(\frac{13}{3}\right)^{0.3}\left(\frac{2600}{430}\right)\left(\frac{1}{48,000}\right)^{0.25} = 0.634 \text{ lanes} \quad \text{(controls)}$$

ii. Exterior girder (AASHTO Table 4.6.2.2.2d-1):

$$g_M = \frac{W_e}{4300} = \frac{2600}{4300} = 0.605 \text{ lanes}$$

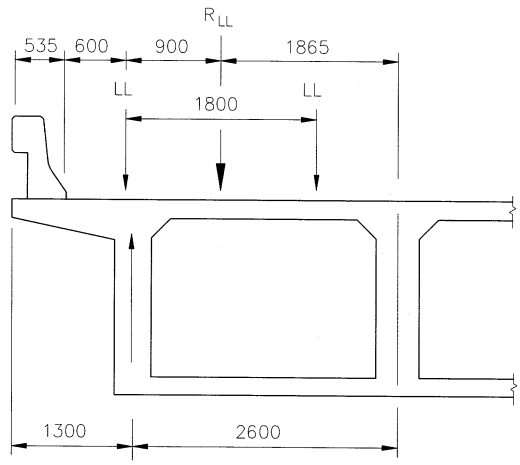

FIGURE 10.13 Live–load distribution for exterior girder — lever rule.

b. *Live-load distribution factor for shear*:

i. Interior girder (AASHTO Table 4.62.2.3a-1):

- One design lane loaded:

$$g_V = \left(\frac{S}{2900}\right)^{0.6}\left(\frac{d}{L}\right)^{0.1}$$

$$= \left(\frac{2600}{2900}\right)^{0.6}\left(\frac{1920}{48,000}\right)^{0.1} = 0.679 \text{ lanes}$$

- Two or more design lanes loaded:

$$g_V = \left(\frac{S}{2200}\right)^{0.9}\left(\frac{d}{L}\right)^{0.1}$$

$$= \left(\frac{2600}{2200}\right)^{0.9}\left(\frac{1920}{48,000}\right)^{0.1} = 0.842 \text{ lanes} \qquad \text{(controls)}$$

ii. Exterior girder (AASHTO Table 4.62.2.3b-1):

- One design lane loaded — Lever rule:
  The lever rule assumes that the deck in its transverse direction is simply supported by the girders and uses statics to determine the live-load distribution to the girders. AASHTO-LRFD [4] also requires that when the lever rule is used, the multiple presence factor m should apply. For a one design lane loaded, $m = 1.2$. The lever rule model for the exterior girder is shown in Figure 10.13. From static equilibrium:

$$R = \frac{965 + 900}{2600} = 0.717$$

$$g_v = mR = 1.2(0.717) = 0.861 \qquad \text{(controls)}$$

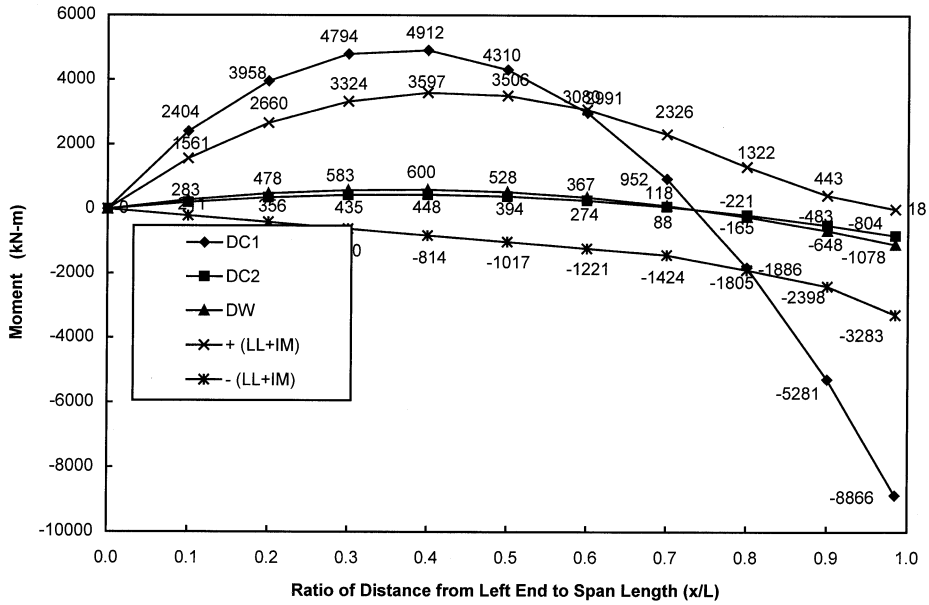

FIGURE 10.14 Moment envelopes for Span 1.

- Two or more design lanes loaded — Modify interior girder factor by e:

$$g_V = eg_{V(\text{interior girder})} = \left(0.64 + \frac{d_e}{3800}\right) g_{V(\text{interior girder})}$$

$$= \left(0.64 + \frac{765}{3800}\right)(0.842) = 0.708 \text{ lanes}$$

- The live load distribution factors at the strength limit state:

Strength Limit State I	Interior Girder	Exterior Girder
Bending moment	0.634 lanes	0.605 lanes
Shear	0.842 lanes	0.861 lanes

5. **Calculate Unfactored Moments and Shear Demands for Interior Girder**
   It is practically assumed that all dead loads are carried by the box girder and equally distributed to each girder. The live loads take forces to the girders according to live load distribution factors (AASHTO Article 4.6.2.2.2). Unfactored moment and shear demands for an interior girder are shown in Figures 10.14 and 10.15. Details are listed in Tables 10.11 and 10.12. Only the results for Span 1 are shown in these tables and figures since the bridge is symmetrical about the bent.

6. **Determine Load Factors for Strength Limit State I and Service Limit State I**
   a. *General design equation* (ASHTO Article 1.3.2):

$$\eta \sum \gamma_i Q_i \leq \phi R_n \tag{10.53}$$

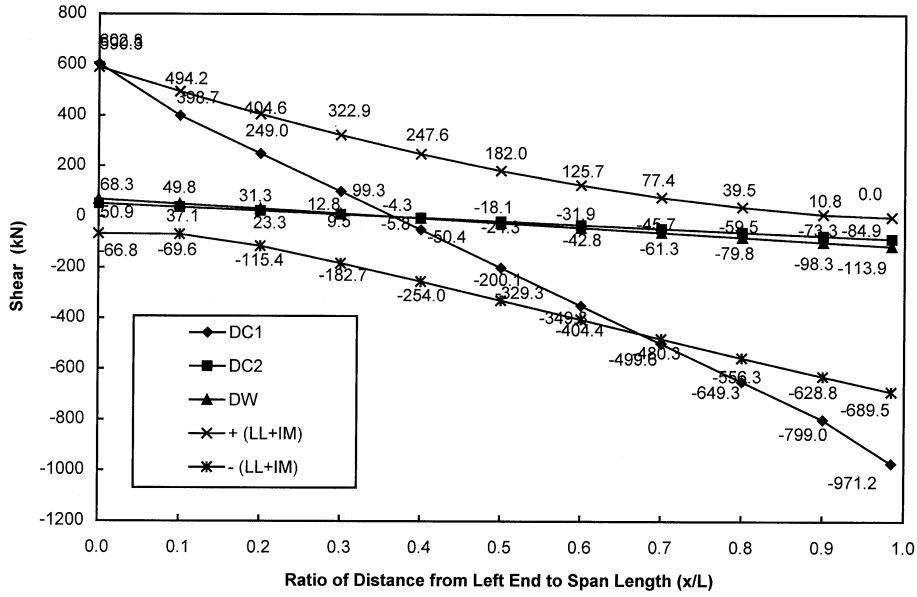

FIGURE 10.15 Shear envelopes for Span 1

TABLE 10.11 Moment and Shear due to Unfactored Dead Load for the Interior Girder

		Unfactored Dead Load					
		*DC*1		*DC*2		DW	
Span	Location (*x*/*L*)	M_{DC1} (kN-m)	V_{DC1} (kN)	M_{DC2} (kN-m)	V_{DC2} (kN)	M_{DW} (kN-m)	V_{DW} (kN)
	0.0	0	603	0	51	0	68
	0.1	2404	399	211	37	283	50
	0.2	3958	249	356	23	478	31
	0.3	4794	99	435	10	583	13
1	0.4	4912	–50	448	–4	600	–6
	0.5	4310	–200	394	–18	528	–24
	0.6	2991	–350	274	–32	367	–43
	0.7	952	–500	88	–46	118	–61
	0.8	–1805	–649	–165	–59	–221	–80
	0.9	–5281	–799	–483	–73	–648	–98
	Face of column	–8866	–971	–804	–85	–1078	–114

Note:
1. *DC*1 — interior girder self-weight.
2. *DC*2 — barrier self-weight.
3. *DW* — wearing surface load.
4. Moments in Span 2 are symmetrical about the bent.
5. Shears in span are anti-symmetrical about the bent.

where γ_i are load factors and ϕ a resistance factor; Q_i represents force effects; R_n is the nominal resistance; η is a factor related to the ductility, redundancy, and operational importance of that being designed and is defined as:

$$\eta = \eta_D \eta_R \eta_I \geq 0.95 \tag{10.54}$$

TABLE 10.12 Moment and Shear Envelopes and Associated Forces for the Interior Girder due to AASHTO HL-93 Live Load

Span	Location (x/L)	Positive Moment and Associated Shear		Negative Moment and Associated Shear		Shear and Associated Moment	
		M_{LL+IM} (kN-m)	V_{LL+IM} (kN)	V_{LL+IM} (kN)	M_{LL+IM} (kN-m)	V_{LL+IM} (kN)	M_{LL+IM} (kN-m)
	0.0	0	259	0	–255	497	0
	0.1	1561	312	–203	–42	416	1997
	0.2	2660	249	–407	–42	341	3270
	0.3	3324	47	–610	–42	272	3915
1	0.4	3597	108	–814	–42	–214	3228
	0.5	3506	–25	–1017	–42	–277	3272
	0.6	3080	–81	–1221	–42	–341	2771
	0.7	2326	–258	–1424	–42	–404	1956
	0.8	1322	–166	–1886	–68	–468	689
	0.9	443	–112	–2398	–141	–529	–945
	Face of column	18	–97	–3283	–375	–581	–1850

Note:
1. *LL + IM* — AASHTO HL-93 live load plus dynamic load allowance.
2. Moments in Span 2 are symmetrical about the bent.
3. Shears in Span 2 are antisymmetrical about the bent.
4. Live load distribution factors are considered.

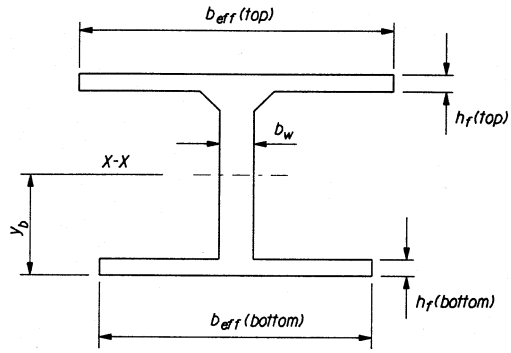

FIGURE 10.16 Effective flange width of interior girder.

For this bridge, the following values are assumed:

Limit States	Ductility η_D	Redundancy η_R	Importance η_I	η
Strength limit state	0.95	0.95	1.05	0.95
Service limit state	1.0	1.0	1.0	1.0

b. *Load factors and load combinations*:
The load factors and combinations are specified as (AASHTO Table 3.4.1-1):
Strength Limit State I: $1.25(DC1 + DC2) + 1.5(DW) + 1.75(LL + IM)$
Service Limit State I: $DC1 + DC2 + DW + (LL + IM)$

7. Calculate Section Properties for Interior Girder
For an interior girder as shown in Figure 10.16, the effective flange width b_{eff} is determined (AASHTO Article 4.6.2.6) by:

TABLE 10.13 Effective Flange Width and Section Properties for Interior Girder

Location	Dimension	Mid span	Bent (face of support)
Top flange	h_f (mm)	200	200
	$L_{eff}/4$ (mm)	9,000	11,813
	$12h_f + b_w$ (mm)	2,700	2,700
	S (mm)	2,600	2,600
	b_{eff} (mm)	**2,600**	**2,600**
Bottom flange	h_f (mm)	150	300
	$L_{eff}/4$ (mm)	9,000	11,813
	$12h_f + b_w$ (mm)	2,100	3,900
	S (mm)	2,600	2,600
	b_{eff} (mm)	**2,100**	**2,600**
Area	A (m^2)	1.316	1.736
Moment of inertia	I (m^4)	0.716	0.968
Center of gravity	y_b (m)	1.085	0.870

Note: L_{eff} = 36.0 m for midspan; L_{eff} = 47.25 m for the bent; b_w = 300 mm.

$$b_{eff} = \text{the lesser of} \begin{cases} \dfrac{L_{eff}}{4} \\ 12h_f + b_w \\ S \end{cases} \tag{10.55}$$

where L_{eff} is the effective span length and may be taken as the actual span length for simply supported spans and the distance between points of permanent load inflection for continuous spans; h_f is the compression flange thickness and b_w is the web width; and S is the average spacing of adjacent girders. The calculated effective flange width and the section properties are shown in Table 10.13 for the interior girder.

8. Calculate Prestress Losses

For a CIP post-tensioned box girder, two types of losses, instantaneous losses (friction, anchorage set, and elastic shortening) and time-dependent losses (creep and shrinkage of concrete, and relaxation of prestressing steel), are significant. Since the prestress losses are not symmetrical about the bent for this bridge, the calculation is performed for both spans.

a. *Frictional loss* Δf_{pF}:

$$\Delta f_{pF} = f_{pj}\left(1 - e^{-(Kx + \mu\alpha)}\right) \tag{10.56}$$

where K is the wobble friction coefficient = 6.6×10^{-7}/mm and μ is the coefficient of friction = 0.25 (AASHTO Article 5.9.5.2.2b); x is the length of a prestressing tendon from the jacking end to the point considered; α is the sum of the absolute values of angle change in the prestressing steel path from the jacking end.

For a parabolic cable path (Figure 10.17), the angle change is $\alpha = 2e_p/L_p$, where e_p is the vertical distance between two control points and L_p is the horizontal distance between two control points. The details are given in Table 10.14.

b. *Anchorage set loss* Δf_{pA}:

For an anchor set thickness of ΔL = 10 mm and E = 200,000 MPa, consider the point D where L_{pF} = 48 m and Δf_{pF} = 96.06 MPa:

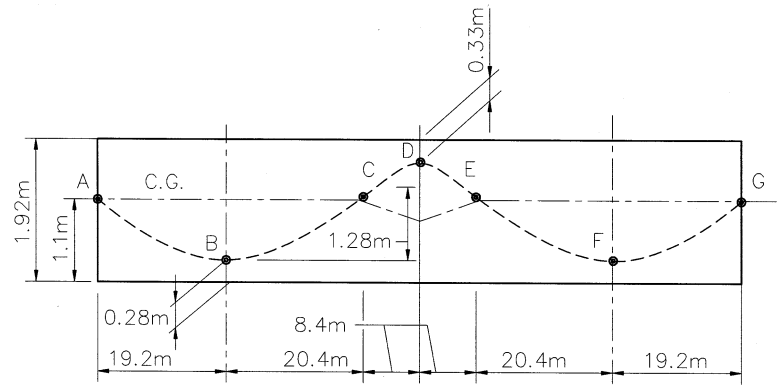

FIGURE 10.17 Parabolic cable path.

TABLE 10.14 Prestress Frictional Loss

Segment	e_p (mm)	L_p (m)	α (rad)	$\Sigma\alpha$ (rad)	ΣL_b (m)	Point	Δf_{pF} (Mpa)
A	0.00	0	0	0	0	A	0.00
AB	820	19.2	0.0854	0.0854	19.2	B	31.44
BC	926	20.4	0.0908	0.1762	39.6	C	64.11
CD	381	8.4	0.0908	0.2669	48.0	D	96.06
DE	381	8.4	0.0908	0.3577	56.4	E	127.28
EF	926	20.4	0.0908	0.4484	76.8	F	157.81
FG	820	19.2	0.0854	0.5339	96.0	G	185.91

$$L_{pA} = \sqrt{\frac{E\,(\Delta L)\,L_{pF}}{\Delta f_{pF}}} = \sqrt{\frac{200{,}000(10)(48{,}000)}{96.06}} = 31\,613 \text{ mm} = 31.6 \text{ m} < 48 \text{ m} \qquad \text{OK}$$

$$\Delta f = \frac{2\,\Delta f_{pF}\,L_{pA}}{L_{pF}} = \frac{2(96.06)(31.6)}{48} = 126.5 \text{ MPa}$$

$$\Delta f_{pA} = \Delta f\left(1 - \frac{x}{L_{pA}}\right) = 126.5\left(1 - \frac{x}{31.6}\right)$$

c. *Elastic shortening loss* Δf_{pES}:
The loss due to elastic shortening in post-tensioned members is calculated using the following formula (AASHTO Article 5.9.5.2.3b):

$$\Delta f_{pES} = \frac{N-1}{2N}\,\frac{E_p}{E_{ci}}\,f_{cgp} \tag{10.57}$$

To calculate the elastic shortening loss, we assume that the prestressing jack force for an interior girder $P_j = 8800$ kN and the total number of prestressing tendons $N = 4$. f_{cgp} is calculated for face of support section:

$$f_{cgp} = \frac{p_j}{A} + \frac{P_j e^2}{I_x} + \frac{M_{DC1} e}{I_x}$$

$$= \frac{8800}{1.736} + \frac{8800\,(0.714)^2}{0.968} + \frac{(-8866)(0.714)}{0.968}$$

$$= 5069 + 4635 - 6540 = 3164 \text{ kN/m}^2 = 3.164 \text{ MPa}$$

$$\Delta f_{pES} = \frac{N-1}{2N} \frac{E_p}{E_{ci}} f_{cgp} = \frac{4-1}{2(4)} \frac{197{,}000}{24768} (3.164) = 9.44 \text{ MPa}$$

d. *Time-dependent losses* Δf_{pTM}:
AASHTO provides a table to estimate the accumulated effect of time-dependent losses resulting from the creep and shrinkage of concrete and the relaxation of the steel tendons. From AASHTO Table 5.9.5.3-1:

$$\Delta f_{pTM} = 145 \text{ MPa} \quad \text{(upper bound)}$$

e. *Total losses* Δf_{pT}:

$$\Delta f_{pT} = \Delta f_{pF} + \Delta f_{pA} + \Delta f_{pES} + \Delta f_{pTM}$$

Details are given in Table 10.15.

9. Determine Prestressing Force P_j for Interior Girder

Since the live load is not in general equally distributed to girders, the prestressing force P_j required for each girder may be different. To calculate prestress jacking force P_j, the initial prestress force coefficient F_{pCI} and final prestress force coefficient F_{pCF} are defined as:

$$F_{pCI} = 1 - \frac{\Delta f_{pF} + \Delta f_{pA} + \Delta f_{pES}}{f_{pj}} \tag{10.58}$$

$$F_{pCF} = 1 - \frac{\Delta f_{pT}}{f_{pj}} \tag{10.59}$$

The secondary moment coefficients are defined as:

$$M_{sC} = \begin{cases} \frac{x}{L} \frac{M_{DA}}{P_j} & \text{for Span 1} \\ \left(1 - \frac{x}{L}\right) \frac{M_{DG}}{P_j} & \text{for Span 2} \end{cases} \tag{10.60}$$

where x is the distance from the left end for each span. The combined prestressing moment coefficients are defined as:

$$M_{psCI} = F_{pCI}(e) + M_{sC} \tag{10.61}$$

TABLE 10.15 Cable Path and Prestress Losses

Span	Location (x/L)	Prestress Losses (MPa) Δf_{pF}	Δf_{pA}	Δf_{pES}	Δf_{pTM}	Δf_{pT}	Force Coefficient F_{pCI}	F_{pCF}
	0.0	0.00	126.50			280.94	0.909	0.811
	0.1	7.92	107.28			269.65	0.916	0.819
	0.2	15.80	88.07			258.31	0.924	0.826
	0.3	23.64	68.85			246.94	0.931	0.834
	0.4	31.44	49.64			235.52	0.939	0.842
1	0.5	39.19	30.42	9.44	145.00	224.06	0.947	0.849
	0.6	46.91	11.21			212.56	0.955	0.857
	0.7	54.58	0.00			209.02	0.957	0.860
	0.8	62.21	0.00			216.65	0.952	0.854
	0.9	77.89	0.00			232.33	0.941	0.844
	1.0	96.06	0.00			250.50	0.929	0.832
	0.0	96.06				250.50	0.929	0.832
	0.1	113.99				268.43	0.917	0.820
	0.2	129.10				283.54	0.907	0.809
	0.3	136.33				290.77	0.902	0.805
2	0.4	143.53	0.00	9.44	145.00	297.97	0.897	0.800
	0.5	150.69				305.13	0.892	0.795
	0.6	157.81				312.25	0.888	0.790
	0.7	164.89				319.33	0.883	0.785
	0.8	171.94				326.38	0.878	0.781
	0.9	178.94				333.38	0.873	0.776
	1.0	185.91				340.35	0.869	0.771

Note: $F_{pCI} = 1 - \dfrac{\Delta f_{pF} + \Delta f_{pA} + \Delta f_{pES}}{f_{pj}}$

$F_{pCF} = 1 - \dfrac{\Delta f_{pT}}{f_{pj}}$

$$M_{psCF} = F_{pCF}(e) + M_{sC} \tag{10.62}$$

where e is the distance between the cable and the center of gravity of a cross section; positive values of e indicate that the cable is above the center of gravity, and negative ones indicate the cable is below the center of gravity of the section.

The prestress force coefficients and the combined moment coefficients are calculated and tabled in Table 10.16. According to AASHTO, the prestressing force P_j can be determined using the concrete tensile stress limit in the precompression tensile zone (see Table 10.5):

$$f_{DC1} + f_{DC2} + f_{DW} + f_{LL+IM} + f_{psF} \geq -0.5\sqrt{f_c'} \tag{10.63}$$

in which

$$f_{DC1} = \frac{M_{DC1}C}{I_x} \tag{10.64}$$

$$f_{DC2} = \frac{M_{DC2}C}{I_x} \tag{10.65}$$

TABLE 10.16 Prestress Force and Moment Coefficients

Span	Location (x/L)	Cable Path e (m)	Force Coefficients		Moment Coefficients (m)				
			F_{pCI}	F_{pCF}	$F_{pCI}e$	$F_{pCF}e$	M_{sC}	M_{psCI}	M_{psCF}
	0.0	0.015	0.909	0.811	0.014	0.012	0.000	0.014	0.012
	0.1	–0.344	0.916	0.819	–0.315	–0.281	0.034	–0.281	–0.247
	0.2	–0.600	0.924	0.826	–0.554	–0.496	0.068	–0.486	–0.428
	0.3	–0.754	0.931	0.834	–0.702	–0.629	0.102	–0.600	–0.526
	0.4	–0.805	0.939	0.842	–0.756	–0.678	0.136	–0.620	–0.541
1	0.5	–0.754	0.947	0.849	–0.714	–0.640	0.171	–0.543	–0.470
	0.6	–0.600	0.955	0.857	–0.573	–0.514	0.205	–0.368	–0.310
	0.7	–0.344	0.957	0.860	–0.329	–0.295	0.239	–0.090	–0.057
	0.8	0.015	0.952	0.884	0.014	0.013	0.273	0.287	0.286
	0.9	0.377	0.941	0.844	0.355	0.318	0.307	0.662	0.625
	1.0	0.717	0.929	0.832	0.666	0.596	0.341	1.007	0.937
	0.0	0.717	0.929	0.832	0.666	0.596	0.347	1.013	0.943
	0.1	0.377	0.917	0.820	0.346	0.309	0.312	0.658	0.622
	0.2	0.015	0.907	0.809	0.014	0.012	0.278	0.291	0.290
	0.3	–0.344	0.902	0.805	–0.310	–0.277	0.243	–0.067	–0.034
	0.4	–0.600	0.897	0.800	–0.538	–0.480	0.208	–0.330	–0.272
2	0.5	–0.754	0.892	0.795	–0.673	–0.599	0.174	–0.499	–0.426
	0.6	–0.805	0.888	0.790	–0.715	–0.636	0.139	–0.576	–0.497
	0.7	–0.754	0.883	0.785	–0.665	–0.592	0.104	–0.561	–0.488
	0.8	–0.600	0.878	0.781	–0.527	–0.468	0.069	–0.457	–0.399
	0.9	–0.344	0.873	0.776	–0.300	–0.267	0.035	–0.266	–0.232
	1.0	0.015	0.869	0.771	0.013	0.012	0.000	0.013	0.012

Note: e is distance between cable path and central gravity of the interior girder cross section, positive means cable is above the central gravity, and negative indicates cable is below the central gravity.

$$f_{DW} = \frac{M_{DW}C}{I_x} \tag{10.66}$$

$$f_{LL+IM} = \frac{M_{LL+IM}C}{I_x} \tag{10.67}$$

$$f_{psF} = \frac{P_{pe}}{A} + \frac{(P_{pe}e)C}{I_x} + \frac{M_sC}{I_x} = \frac{F_{pCF}P_j}{A} + \frac{M_{psCF}P_jC}{I_x} \tag{10.68}$$

where C (= y_b or y_t) is the distance from the extreme fiber to the center of gravity of the cross section. f_c' is in MPa and P_{pe} is the effective prestressing force after all losses have been incurred. From Eqs. (10.63) and (10.68), we have

$$P_j = \frac{-f_{DC1} - f_{DC2} - f_{DW} - f_{LL+IM} - 0.5\sqrt{f_c'}}{\dfrac{F_{pCF}}{A} + \dfrac{M_{psCF}C}{I_x}} \tag{10.69}$$

Detailed calculations are given in Table 10.17. Most critical points coincide with locations of maximum eccentricity: $0.4L$ in Span 1, $0.6L$ in Span 2, and at the bent. For this bridge, the controlling section is through the right face of the bent. Herein, P_j = 8741 kN. Rounding P_j up to 8750 kN gives a required area of prestressing steel of $A_{ps} = P_j/f_{pj}$ = 8750/1488 (1000) = 5880 mm^2.

TABLE 10.17 Determination of Prestressing Jacking Force for an Interior Girder

		Top Fiber					Bottom Fiber				
		Stress (MPa)				Jacking Force,	Stress (MPa)				Jacking Force
Span	Location (x/L)	f_{DC1}	f_{DC2}	f_{DW}	f_{LL+IM}	P_j (kN)	f_{DC1}	f_{DC2}	f_{DW}	f_{LL+IM}	P_j(kN)
	0.0	0.000	0.000	0.000	0.000	—	0.000	0.000	0.000	0.000	0
	0.1	2.803	0.246	0.330	1.820	—	–3.642	–0.320	–0.429	–2.365	4405
	0.2	4.616	0.415	0.557	3.103	—	–5.998	–0.540	–0.724	–4.032	6778
	0.3	5.591	0.507	0.680	3.876	—	–7.265	–0.659	–0.884	–5.037	7824
	0.4	5.728	0.522	0.700	4.195	—	–7.442	–0.678	–0.910	–5.450	8101
1	0.5	5.027	0.459	0.616	4.089	—	–6.532	–0.597	–0.800	–5.313	7807
	0.6	3.488	0.319	0.428	3.591	—	–4.532	–0.415	–0.557	–4.667	6714
	0.7	1.110	0.102	0.137	2.712	—	–1.443	–0.133	–0.178	–3.524	3561
	0.8	–2.105	–0.192	–0.258	1.542	2601	2.736	0.250	0.335	–2.004	—
	0.9	–6.159	–0.565	–0.756	0.516	5567	8.003	0.733	0.982	–0.671	—
	1.0	–9.617	–0.872	–1.169	0.020	8406	7.968	0.722	0.969	–0.016	—
	0.0	–9.617	–0.872	–1.169	0.020	8370	7.968	0.722	0.969	–0.016	—
	0.1	–.6.159	–0.564	–0.756	0.516	5661	8.003	0.733	0.982	–0.671	—
	0.2	–2.105	–0.192	–0.258	1.542	2681	2.736	0.250	0.335	–2.004	—
	0.3	1.110	0.102	0.137	2.712	—	–1.443	–0.133	–0.178	–3.524	3974
	0.4	3.488	0.319	0.428	3.591	—	–4.532	–0.415	–0.557	–4.667	7381
2	0.5	5.027	0.459	0.616	4.089	—	–6.532	–0.597	–0.800	–5.313	8483
	0.6	5.728	0.522	0.700	4.195	—	–7.443	–0.678	–0.910	–5.450	**8741**
	0.7	5.591	0.507	0.680	3.876	—	–7.265	–0.659	–0.884	–5.037	8382
	0.8	4.616	0.415	0.557	3.103	—	–5.998	–0.540	–0.724	–4.032	7220
	0.9	2.803	0.246	0.330	1.820	—	–3.642	–0.320	–0.429	–2.365	4666
	1.0	0.000	0.000	0.000	0.000	—	0.000	0.000	0.000	0.000	0

Notes:
1. Positive stress indicates compression and negative stress indicates tension.
2. P_j are obtained by Eq. (10.69).

10. Check Concrete Strength for Interior Girder — Service Limit State I

Two criteria are imposed on the level of concrete stresses when calculating required concrete strength (AASHTO Article 5.9.4.2):

$$\begin{cases} f_{DC1} + f_{psI} \le 0.55 f'_{ci} & \text{at prestressing state} \\ f_{DC1} + f_{DC2} + f_{DW} + f_{LL+IM} + f_{psF} \le 0.45 f'_c & \text{at service state} \end{cases} \tag{10.70}$$

$$f_{psI} = \frac{P_{jI}}{A} + \frac{(P_{jI}e)C}{I_x} + \frac{M_{sI}C}{I_x} = \frac{F_{pCI}P_j}{A} + \frac{M_{psCI}P_jC}{I_x} \tag{10.71}$$

The concrete stresses in the extreme fibers (after instantaneous losses and final losses) are given in Tables 10.18. and 10.19. For the initial concrete strength in the prestressing state, the controlling location is the top fiber at 0.8L section in Span 1. From Eq. (10.70), we have

$$f'_{ci,reg} \ge \frac{f_{DC1} + f_{psI}}{0.55} = \frac{7.15}{0.55} = 13\text{MPa}$$

$$\therefore \quad \underline{\text{use } f'_{ci} = 24 \text{ MPa}} \qquad \text{OK}$$

TABLE 10.18 Concrete Stresses after Instantaneous Losses for the Interior Girder

Span	Location (x/L)	Top Fiber Stress (MPa) f_{DC1}	F_{pC1^*} P_j/A	M_{psC1^*} $P_j^* Y_t/I$	f_{psI}	Total Initial Stress	Bottom Fiber Stress (MPa) f_{DC1}	F_{pC1^*} P_j/A	M_{psC1^*} $P_j^* Y_t/I$	f_{psI}	Total Initial Stress
	0.0	0.00	6.04	0.14	6.18	6.18	0.00	6.04	–0.18	5.86	5.86
	0.1	2.80	6.09	–2.87	3.23	6.03	–3.64	6.09	3.72	9.82	6.17
	0.2	4.62	6.14	–4.96	1.18	5.80	–6.00	6.14	6.45	12.59	6.59
	0.3	5.59	6.19	–6.12	0.07	5.66	–7.27	6.19	7.95	14.15	6.88
	0.4	5.73	6.24	–6.32	–0.08	5.65	–7.44	6.24	8.22	14.46	7.02
1	0.5	5.03	6.30	–5.54	0.75	5.78	–6.53	6.30	7.20	13.50	6.97
	0.6	3.49	6.35	–3.76	2.59	6.08	–4.53	6.35	4.88	11.23	6.70
	0.7	1.11	6.36	–0.92	5.44	6.55	–1.44	6.36	1.20	7.56	6.12
	0.8	–2.11	6.33	2.93	9.26	**7.15**	2.74	6.33	–3.81	2.52	5.26
	0.9	–6.16	6.26	6.76	13.02	6.86	8.00	6.26	–8.78	–2.52	5.48
	1.0	–9.62	4.68	9.56	14.24	4.62	7.97	4.68	–7.92	–3.24	4.73
	0.0	–9.62	4.68	9.62	14.30	4.68	7.97	4.68	–7.97	–3.28	4.68
	.1	–6.16	6.10	6.72	12.82	6.66	8.00	6.10	–8.73	–2.63	5.37
	0.2	–2.11	6.03	2.97	9.00	6.90	2.74	6.03	–3.86	2.17	4.90
	0.3	1.11	6.00	–0.69	5.31	6.42	–1.44	6.00	0.89	6.89	5.45
	0.4	3.49	5.97	–3.37	2.60	6.08	–4.53	5.97	4.38	10.34	5.81
2	0.5	5.03	5.93	–5.09	0.84	5.87	–6.53	5.93	6.62	12.55	6.02
	0.6	5.73	5.90	–5.87	0.03	5.75	–7.44	5.90	7.63	13.54	6.09
	0.7	5.59	5.87	–5.73	0.14	5.73	–7.27	5.87	7.44	13.31	6.05
	0.8	4.62	5.84	–4.67	1.71	5.79	–6.00	5.84	6.07	11.90	5.91
	0.9	2.80	5.81	–2.71	3.10	5.90	–3.64	5.81	3.52	9.33	5.69
	1.0	0.00	5.78	0.13	5.91	5.91	0.00	5.78	–0.17	5.60	5.60

Note: Positive stress indicates compression and negative stress indicates tension

For the final concrete strength at the service limit state, the controlling location is in the top fiber at 0.6L section in Span 2. From Eq. (10.70), we have

$$f'_{c,req} \geq \frac{f_{DC1} + f_{DC2} + f_{DW} + f_{LL+IM} + f_{psF}}{0.45} = \frac{11.32}{0.45} = 21.16 \text{ MPa} < 28 \text{MPa}$$

$$\therefore \quad \underline{\text{choose } f'_c = 28 \text{MPa}} \qquad \text{OK}$$

11. Flexural Strength Design for Interior Girder — Strength Limit State I

AASHTO [4] requires that for the Strength Limit State I

$$M_u \leq \phi M_n$$

$$M_u = \eta \sum \gamma_i M_i = 0.95[1.25(M_{DC1} + M_{DC2}) + 1.5M_{DW} + 1.75M_{LLH}] + M_{ps}$$

where ϕ is the flexural resistance factor 1.0 and M_{ps} is the secondary moment due to prestress. Factored moment demands M_u for the interior girder in Span 1 are calculated in Table 10.20. Although the moment demands are not symmetrical about the bent (due to different secondary prestress moments), the results for Span 2 are similar and the differences will not be considered in this example. The detailed calculations for the flexural resistance ϕM_n are shown in Table 10.21. It is seen that no additional mild steel is required.

TABLE 10.19 Concrete Stresses after Total Losses for the Interior Girder

Span	Location (x/L)	Top Fiber Stress (MPa) f_{LOAD}	F_{pCF^*} $P_{j/A}$	M_{psCF^*} $P_{j^*Yt/I}$	f_{psF}	Total Final Stress	Bottom Fiber Stress (MPa) f_{LOAD}	F_{pCF^*} $P_{j/A}$	M_{psCF^*} P_{j^*yb}/I	f_{psF}	Total Final Stress
	0.0	0.00	5.39	0.12	5.52	5.52	0.00	5.39	–0.16	5.23	5.23
	0.1	5.20	5.44	–2.52	2.92	8.12	–6.76	5.44	3.28	8.72	1.97
	0.2	8.69	5.49	–4.36	1.13	9.82	–11.29	5.49	5.67	11.16	–0.13
	0.3	10.66	5.55	–5.37	0.17	10.83	–13.85	5.55	6.98	12.52	–1.32
	0.4	11.14	5.60	–5.52	0.07	11.22	–14.48	5.60	7.18	12.77	–1.71
1	0.5	10.19	5.65	–4.79	0.85	11.05	–13.24	5.65	6.23	11.88	–1.37
	0.6	7.83	5.70	–3.16	2.54	10.37	–10.17	5.70	4.11	9.81	–0.36
	0.7	4.06	5.71	–0.58	5.14	9.20	–5.28	5.71	0.75	6.47	1.19
	0.8	–4.75	5.68	2.91	8.60	3.84	6.18	5.68	–3.79	1.89	8.07
	0.9	–10.28	5.61	6.38	11.99	1.72	13.35	5.61	–8.29	–2.68	10.67
	1.0	–15.22	4.19	8.90	13.09	–2.13	12.61	4.19	–7.37	–3.18	9.43
	0.0	–15.22	4.19	8.95	13.14	–2.07	12.61	4.19	–7.42	–3.23	9.38
	0.1	–10.28	5.45	6.34	11.79	1.52	13.35	5.45	–8.24	–2.79	10.56
	0.2	–4.75	5.38	2.96	8.34	3.58	6.18	5.38	–3.84	1.54	7.72
	0.3	4.06	5.35	0.34	5.01	9.07	–5.28	5.35	0.45	5.80	0.52
	0.4	7.83	5.32	–2.77	2.55	10.37	–10.17	5.32	3.60	8.92	–1.25
2	0.5	10.19	5.29	–4.34	0.94	11.13	–13.24	5.29	5.64	10.93	–2.31
	0.6	11.14	5.25	–5.07	0.18	**11.32**	–14.48	5.25	6.59	11.85	**–2.63**
	0.7	10.66	5.22	–4.98	0.24	10.90	–13.85	5.22	6.47	11.69	–2.15
	0.8	8.69	5.19	–4.07	1.12	9.81	–11.29	5.19	5.29	10.48	–0.81
	0.9	5.20	5.16	–2.37	2.79	7.99	–6.76	5.16	3.08	8.24	1.48
	1.0	0.00	5.13	0.12	5.25	5.25	0.00	5.13	–0.15	4.97	4.97

Notes:
1. $f_{LOAD} = f_{DC1} + f_{DC2} + f_{DW} + f_{LL+IM.}$
2. Positive stress indicates compression and negative stress indicates tension.

TABLE 10.20 Factored Moments for an Interior Girder

Span	Location (x/L)	M_{DC1} (kN-m) Dead Load 1	M_{DC2} (kN-m) Dead Load 2	M_{DW} (kN-m) Wearing Surface	M_{LL+IM} (kN-m) Positive	M_{LL+IM} (kN-m) Negative	M_{ps} (kN-m) P/S	M_u (kN-m) Positive	M_u (kN-m) Negative
	0.0	0	0	0	0	0	0	**0**	0
	0.1	2404	211	283	1561	–203	298	**6,402**	3,469
	0.2	3958	356	478	2660	–407	597	**10,824**	5,725
	0.3	4794	435	583	3324	–610	895	**13,462**	6,922
	0.4	4912	448	600	3597	–814	1194	**14,393**	7,060
1	0.5	4310	395	528	3506	–1017	1492	**13,660**	6,140
	0.6	2991	274	367	3080	–1221	1790	**11,310**	4,161
	0.7	952	88	118	2326	–1424	2089	**7,358**	1,124
	0.8	–1805	–165	–221	1322	–1886	2387	1,931	**3,403**
	0.9	–5281	–483	–648	443	–2398	2685	–4.348	**9,071**
	1.0	–8866	–804	–1078	18	–3283	2984	–10,005	**–15,492**

Note: $M_u = 0.95[1.25(M_{DC1} + M_{DC2}) + 1.5M_{DW} + 1.75M_{LL+IM}] + M_{ps}$.

12. Shear Strength Design for Interior Girder — Strength Limit State I

AASHTO [4] requires that for the strength limit state I

$$V_u \leq \phi V_n$$

$$V_u = \eta \sum \gamma_i V_i = 0.95[1.25(V_{DC1} + V_{DC2}) + 1.5V_{DW} + 1.75V_{LL+IM}] + V_{ps}$$

TABLE 10.21 Flexural Strength Design for Interior Girder — Strength Limit State I

Span	Location (x/L)	A_{ps} mm²	d_p mm	A_s mm²	d_s mm	b mm	c mm	f_{ps} Mpa	d_e mm	a mm	ϕM_n Mpa	M_u kN-m
	0.0		32.16	0	72.06	104	7.14	253.2	32.16	6.07	5,206	0
	0.1		46.09	0	72.06	104	7.27	258.1	46.09	6.18	7,833	4,009
	0.2		56.04	0	72.06	104	7.33	260.1	56.04	6.23	9,717	6,820
	0.3		61.54	0	72.06	104	7.35	261.0	61.54	6.25	10,759	8,469
	0.4		64.00	0	72.06	104	7.36	261.3	64.00	6.26	11,226	9,012
1	0.5	8.47	62.29	0	72.06	104	7.36	261.1	62.29	6.25	10,903	8,494
	0.6		57.20	0	72.06	104	7.34	260.3	57.20	6.24	9,937	6,942
	0.7		48.71	0	72.06	104	7.29	258.7	48.71	6.20	8,328	4,392
	0.8		38.20	0	71.06	82.5	21.19	228.1	38.20	18.01	–4,965	–1.397
	0.9		53.48	0	71.06	82.5	23.36	237.0	53.48	19.86	–7,822	–5,906
	1.0		62.00	0	71.06	104	8.13	261.0	62.00	6.25	–10,848	–10,716

TABLE 10.22 Factored Shear for an Interior Girder

Span	Location (x/L)	V_{DC1} (kN) Dead Load 1	V_{DC2} (kN) Dead Load 2	V_{DW} (kN) Wearing Surface	V_{LL+IM} (kN) Envelopes	M_{LL+IM} (kN-m) Associated	V_{ps} (kN) P/S	V_u (kN)	M_u (kN-m) Associated
	0.0	602.8	50.9	68.3	497.0	0.0	62.2	1762.0	0
	0.1	398.7	37.1	49.8	416.1	1997.4	62.2	1342.5	7,128
	0.2	249.0	23.3	31.3	340.7	3270.3	62.2	996.5	11,838
	0.3	99.3	9.5	12.8	271.9	3915.3	62.2	661.6	14,446
	0.4	–50.4	–4.3	–5.8	–213.9	3228.4	62.2	–366.6	13,780
1	0.5	–200.1	–18.1	–24.3	–277.3	3271.7	62.2	–692.6	13,270
	0.6	–349.8	–31.9	–42.8	–340.5	2771.1	62.2	–1018.2	10,797
	0.7	–499.6	–45.7	–61.3	–404.4	1955.7	62.2	–1345.0	6,742
	0.8	–649.3	–59.5	–79.8	–468.4	689.4	62.2	–1671.9	879
	0.9	–799.0	–73.3	–98.3	–529.5	–945.3	62.2	–1994.0	–6,655
	1.0	–971.2	–84.9	–113.9	–580.6	–1849.7	62.2	–2319.5	–13,110

Note: $V_v = 0.95[1.25(V_{DC1} + V_{DC2}) + 1.5V_{DW} + 1.75V_{LL+IM}] + V_{ps}$.

TABLE 10.23 Shear Strength Design for Interior Girder Strength Limit State I

Span	Location (x/L)	d_v (mm)	y' (rad)	V_p (kN)	v/f_c'	ε_x (1000)	θ (°)	β	V_c (kN)	S (mm)	ϕV_n (kN)	$\lvert V_u \rvert$ (kN)
	0.0	1382	0.085	606	0.133	–0.256	21.0	2.68	428	100	1860	1762
	0.1	1382	0.064	459	0.101	–0.382	27.0	5.60	894	300	1513	1342
	0.2	1382	0.043	309	0.078	–6.241	33.0	2.37	378	200	1036	996
	0.3	1503	0.021	156	0.052	–6.299	38.0	2.10	365	300	753	662
	0.4	1555	0.000	0	0.036	–6.357	36.0	2.23	400	600	511	367
1	0.5	1503	0.021	159	0.055	–6.415	36.0	2.23	387	400	710	693
	0.6	1382	0.043	320	0.080	–6.473	30.0	2.48	396	200	1076	1018
	0.7	1382	0.064	482	0.099	–0.401	27.0	5.63	899	300	1538	1345
	0.8	1382	0.085	639	0.120	–0.398	23.5	6.50	1038	300	1813	1672
	0.9	1382	0.091	670	0.152	–6.372	23.5	3.49	557	100	2017	1994
	1.0	1502	0.000	0	0.233	–6.280	36.0	1.00	173	40	2343	2319

where ϕ is shear resistance factor 0.9 and V_{ps} is the secondary shear due to prestress. Factored shear demands V_u for the interior girder are calculated in Table 10.22. To determine the effective web width, assume that the VSL post-tensioning system of 5 to 12 tendon units [VLS, 1994] will be used with a grouted duct diameter of 74 mm. In this example, $b_v = 300 - 74/2 = 263$ mm. Detailed calculations of the shear resistance ϕV_n (using two-leg #15M stirrups $A_v = 400$ mm²) for Span 1 are shown in Table 10.23. The results for Span 2 are similar to Span 1 and the calculations are not repeated for this example.

References

1. Lin, T. Y. and Burns, N. H., *Design of Prestressed Concrete Structure*, 3rd ed., John Wiley & Sons, New York, 1981.
2. Nawy, E. G., *Prestressed Concrete*: *A Fundamental Approach*, 2nd ed., Prentice-Hall, Englewood Cliffs, NJ, 1996.
3. Collins, M. P. and Mitchell, D., *Prestressed Concrete Structures*, Prentice-Hall, Englewood Cliffs, NJ, 1991.
4. AASHTO, *AASHTO LRFD Bridge Design Specifications*, 1st ed., American Association of State Highway and Transportation Officials, Washington, D.C., 1994.
5. PCI, *PCI Design Handbook – Precast and Prestressed Concrete*, 3rd ed., Prestressed Concrete Institute, Chicago, IL, 1985.
6. Eubunsky, I. A. and Rubinsky, A., A preliminary investigation of the use of fiberglass for prestressed concrete, *Mag. Concrete Res.*, Sept., 71, 1954.
7. Wines, J. C. and Hoff, G. C., Laboratory Investigation of Plastic — Glass Fiber Reinforcement for Reinforced and Prestressed Concrete, *Report 1,* U.S. Army Corps of Engineers, Waterway Experimental Station, Vicksburg, MI, 1966.
8. Wines, J. C., Dietz, R. J., and Hawly, J. L., Laboratory Investigation of Plastic — Glass Fiber Reinforcement for Reinforced and Prestressed Concrete, *Report 2,* U.S. Army Corps of Engineers, Waterway Experimental Station, Vicksburg, MI, 1966.
9. Iyer, S.I. and Anigol, M., Testing and evaluating fiberglass, graphite, and steel prestressing cables for pretensioned beams, in *Advanced Composite Materials in Civil Engineering Structures*, Iyer, S. I. and Sen, R., Eds., ASCE, New York, 1991, 44.
10. Miesseler, H. J. and Wolff, R., Experience with fiber composite materials and monitoring with optical fiber sensors, in *Advanced Composite Materials in Civil Engineering Structures*, Iyer, S. I. and Sen, R., Eds., ASCE, New York, 1991, 167–182.
11. Kim, P. and Meier, U., CFRP cables for large structures, in *Advanced Composite Materials in Civil Engineering Structures*, Iyer, S. I. and Sen, R., Eds., ASCE, New York, 1991, 233–244.
12. PTI, *Post-Tensioning Manual*, 3rd ed., Post-Tensioning Institute, Phoenix, AZ, 1981.
13. FHWA, *Standard Plans for Highway Bridges, Vol. I, Concrete Superstructures*, U.S. Department of Transportation, FHWA, Washington, D.C., 1990.
14. ACI, *Building Code Requirements for Structural Concrete (ACI318-95) and Commentary* (ACI318R-95), American Concrete Institute, Farmington Hills, MI, 1995.
15. CEB-FIP, *Model Code for concrete structures.* (MC-90). Comité Euro-international du Béton (CEB)-Fédération Internationale de la précontrainte (FIP) (1990). Thomas Telford, London, U.K. 1993.